PRIFYSGOL BANGOR / BANGOR UNIVERSITY

On the optimization of green multimodal transportation: A case study of the West German canal system

Binsfeld, Tom; Hamdan, Sadeque; Jouini, Oualid; Gast, Johannes

Annals of Operations Research

DOI:
10.1007/s10479-024-06075-5

E-pub ahead of print: 04/06/2024

Peer reviewed version

Cyswllt i'r cyhoeddiad / Link to publication

Dyfyniad o'r fersiwn a gyhoeddwyd / Citation for published version (APA):
Binsfeld, T., Hamdan, S., Jouini, O., & Gast, J. (2024). On the optimization of green multimodal transportation: A case study of the West German canal system. *Annals of Operations Research*. Advance online publication. https://doi.org/10.1007/s10479-024-06075-5

Hawliau Cyffredinol / General rights
Copyright and moral rights for the publications made accessible in the public portal are retained by the authors and/or other copyright owners and it is a condition of accessing publications that users recognise and abide by the legal requirements associated with these rights.

• Users may download and print one copy of any publication from the public portal for the purpose of private study or research.
• You may not further distribute the material or use it for any profit-making activity or commercial gain
• You may freely distribute the URL identifying the publication in the public portal ?

Take down policy
If you believe that this document breaches copyright please contact us providing details, and we will remove access to the work immediately and investigate your claim.

15. Aug. 2024

On the optimization of green multimodal transportation: A case study of the West German canal system

Tom Binsfeld[1,3], Sadeque Hamdan[2*], Oualid Jouini[1], Johannes Gast[3]

[1]Laboratoire Genie Industriel, Université Paris-Saclay, CentraleSupélec, 3 rue Joliot-Curie, Gif-sur-Yvette, 91190, Île-de-France, France.
[2*]Bangor Business School, Bangor University, College Rd, Bangor, LL57 2DG, Gwynedd, United Kingdom.
[3]4flow research, 4flow, Hallerstraße 1, Berlin, 10587, Germany.

*Corresponding author(s). E-mail(s): s.hamdan@bangor.ac.uk;
Contributing authors: t.binsfeld@4flow.com;
oualid.jouini@centralesupelec.fr; johannes.gast@posteo.de;

Abstract

In this study, we address a biobjective multimodal routing problem that consists of selecting transportation modes and their respective quantities, optimizing transshipment locations, and allocating port orders. In the objective functions, we minimize total transportation costs and use the EcoTransit methodology to minimize total greenhouse gas emissions. The optimization model selects the transportation mode and transshipment port where quantities are transshipped from one mode to another. We compare inland waterway transportation and trucks encountering infrastructure failures that require rerouting or modal shifting in a real-life case study on the supply of goods for the chemical industry in the West German canal system. We propose a population-based heuristic to solve large instances in a reasonable computation time. A sensitivity analysis of demand, of varying lock times, and of infrastructure failure scenarios was conducted. We show that compared with inland waterway transportation, multimodal transportation reduces costs by 23% because of longer lock times. Our analysis shows that the use of inland waterway transportation only during infrastructure failures imposes nearly 28% higher costs per day depending on the failure location compared to that of the case of no failures. We also show that the use

of a multimodal transportation system helps to reduce this cost increase in lock failure scenarios.

Keywords: Multimodal transportation, Inland waterway transport, Greenhouse gas emissions, Sustainability, Vehicle routing, Modal shift, Optimization

1 Introduction

While the need for energy security has induced pressure on economies and societies in 2024, inland waterways ensure a scalable supply of energy feedstock. Under typical operating conditions, waterways are reliable and flexible transport systems based on an efficient infrastructure (Federal Ministry of Transport and Digital Infrastructure, 2019). However, extreme weather and dilapidated infrastructure threaten the availability of waterways for freight transport in Germany. Approximately 18 million tons of goods are transported monthly on German inland waterways depending on their availability. This volume equates to more than two million long-haul truckloads (Federal Office of Statistics, 2019). In general, public authorities aspire to further utilize existing capacity reserves of this environmentally friendly mode of transport; the plan is to shift traffic from roads to inland waterways: The European Union is pursuing the target of doubling their modal shift share up to 9% in 2030, as aligned with the German "Masterplan Binnenschiff" from the German Federal Ministry of Transport and Digital Infrastructure (Sims et al., 2014).

Overall, inland waterway transport represents an elementary component of the German and European logistical supply chains. Nonetheless, inland barges cannot serve and satisfy the logistical requirements of every industry. Other transportation modes, such as trucks, promise greater flexibility and availability while not requiring dedicated infrastructure (i.e., ports and canals). Evolving risks, such as infrastructure failures or climate change, among others, also impact transportation mode choice. Hence, multimodal transport is often established to exploit the advantages of each mode.

Infrastructure failures, such as lock failures or bridge damage, are the main reasons for the nonavailability of whole canal sections, resulting in specific ports becoming temporarily unavailable (Gast, Wehrle, Wiens, & Schultmann, 2020). This unavailability has caused significant (economic) damage to companies. For example, the low amount of water on the Rhine River in 2018 induced a cost of €245 million for a chemical company in Germany (Reuters, 2019). Moreover, these risks lead to higher costs, higher emissions, and missing the time schedule; such issues can incur additional costs in the downstream supply chain. These observations highlight the need for a novel multimodal concept to ensure good flow along the supply chain, regardless of the availability of primary transportation infrastructure at the time.

In this study, we formulate an optimization problem that addresses these issues. In this formulation, different transportation modes can be used either directly from the depot or at any port that acts as a transshipment port, where quantities unloaded by one mode are shifted to another mode of transportation. The problem is formulated

as a biobjective mathematical model in which we minimize the total transportation cost and the greenhouse gas emissions of the network system. The proposed mixed-integer linear model helps decision-makers to identify the optimal route for each transportation mode and each vehicle, the quantity transported by each vehicle and each transportation mode, the location of the transshipment port, and the quantity shifted from one mode to another. We demonstrate how this multimodal consideration can be reduced to a single-mode optimization model. We combine the advantages of different transportation modes and develop an optimization tool to determine the optimal transportation mode. The problem is *NP*-hard, as we show in Section A of the Appendix. Therefore, we propose a population-based heuristic to solve this problem. The heuristics generate a set of feasible individuals, and the model attempts to improve these individuals in each iteration by using 18 operators. We also compare different scenarios by using single and multiple modes. Furthermore, we analyze the impact of different scenarios on the transport of chemical goods in the West German canal system in a case study.

This study provides the following contributions. We optimized the selection of transshipment ports that can be used for both loading and unloading in this setting, which is inspired by a real-world problem, given the multimodal choice of either truck or inland waterway transportation. This type of problem has received limited attention in the literature. Furthermore, we allow for different types of vehicles to be chosen; in the literature, the focus has been on a single-vehicle type in multimodal problems. By adding a virtual port to act as a depot, our approach maintains model linearity; this approach avoids further complexity in this *NP*-hard problem. We use a biobjective formulation to model the potentially conflicting objectives of cost reduction and reduction of greenhouse gas emissions, with emissions calculated by using the EcoTransit methodology. Although this problem can still be solved in an acceptable runtime for small to medium instances, solving large instances optimally becomes infeasible. To address this issue, we developed a particular population-based heuristic that performs well, with less than 5% error from the best exact solution found and more than 83% time savings in most cases. We derive several managerial insights by using a practical case study from the research project *Preview*. In this project, we assess the vulnerability and the resilience of supply chains that depend on the infrastructure of the West German canal systems by mainly requiring inland waterway transport. We highlight the benefits of multimodal transportation over single-mode transportation in terms of cost and emissions under various scenarios. The scenarios vary in terms of lock time, demand, and whether infrastructure failure occurs. Interestingly, it appears that the use of multimodal transportation reduces the impact of increasing lock times; moreover, multimodal transportation allows for savings in the case of infrastructure failure. This demonstrates the economic effectiveness of rerouting and modal shifts as risk-mitigation strategies for supply chains. We calculated the cost of reducing emissions by using each transportation model, and we showed that the multimodal transportation mode provides a faster reduction rate of 1.12% of emissions for each 1% increase in the costs.

The remainder of this study is organized as follows. In Section 2, we review the relevant work related to this study. In Section 3, we describe the methodology used

in this study. Section 4 contains the solution approach. In Section 5, we present a case study, and in Section 6, we describe the numerical experiments related to the proposed heuristic. Section 7 provides managerial insights. Finally, Section 8 concludes the paper, and we highlight future research avenues.

2 Literature Review

The multimodal transportation model is a routing problem variant that uses multiple vehicles and different transportation modes. The use of multiple vehicles is similar to the multiple traveling salesman problem (m-TSP), which is a generalization of the TSP problem, which originally includes only one vehicle (salesperson). One important feature of the multimodal problem is the use of a transshipment point, where quantities are transferred from one mode to another. Therefore, in this section we review the related literature. First, we discuss different routing model variants. Then, we review works that focus on multimodal transportation and provide context for our work within the literature.

2.1 Routing model variants and solution algorithms

The TSP is a fundamental routing challenge to find the shortest optimal routes to minimize travel costs. First introduced in the 1930s and extensively analyzed since then, the TSP requires finding a sequence for a salesperson to visit a set of nodes exactly once, starting and ending at a depot (Miller, Tucker, & Zemlin, 1960). Gutin and Punnen (2006) offered an overview up to 2006, highlighting the broad applicability of the TSP and the emergence of many variants. The m-TSP, involving multiple salespeople, is determine the optimal sequence for multiple vehicles, with each salesman visiting a subset of nodes exactly once (Miller et al., 1960). Rao (1980) explored both symmetric and asymmetric m-TSPs and compared their transformations. The VRP, which is closely related to the TSP, differs in that it seeks sequences for vehicles while considering their capacity. Variants include simultaneous pick-up and delivery (Min, 1989), split pick-up m-VRP (Lee, Epelman, White III, & Bozer, 2006), and multidepot m-VRP with fuel constraints (Sundar, Venkatachalam, & Rathinam, 2016). A two-echelon multivehicle location-routing problem with time windows was introduced by Govindan, Jafarian, Khodaverdi, and Devika (2014), and a hybrid multiobjective multidepot VRP was developed by Londoño, González, Giraldo, and Escobar (2024) to minimize the distance and the control route length standard deviation. Other interesting variants include the railway TSP, where salespeople utilize railways to minimize travel time, considering trains' schedules and nonstop routes (Hadjicharalambous, Pop, Pyrga, Tsaggouris, & Zaroliagis, 2007), and the colored TSP and colored bottleneck TSP, which address multimachine engineering system planning problems (Dong & Cai, 2019; Dong, Lin, Shen, Guo, & Li, 2023).

The traveling purchaser problem (TPP), a routing and purchasing challenge, involves visiting suppliers to buy products at varying prices to satisfy demand at the lowest cost. The TPP is distinguished by the need to minimize both traveling and purchasing costs, making the problem more complex (Cheaitou, Hamdan, Larbi, & Alsyouf, 2021). Variants of the TPP include deterministic, biobjective, and budget

constraints or total quantity discounts (Manerba & Mansini, 2012; Manerba, Mansini, & Riera-Ledesma, 2017; Ravi & Salman, 1999; Riera-Ledesma & Salazar-González, 2005). Finally, the Family TSP is focused on minimizing costs to visit a predetermined number of cities, requiring decisions on which cities to visit within each group (Bernardino & Paias, 2018). For further exploration of variants such as quota, profit-based, and time window TSPs, readers can refer to Ilavarasi and Joseph (2014); Pop, Cosma, Sabo, and Sitar (2024).

The TSP and its variants, which are strongly *NP*-hard, have prompted researchers to develop various heuristics for efficient solution finding. Xing and Tu (2020) employed a Monte Carlo tree search to offer an alternative to traditional exact methods for the TSP. For clustered cities, Jafarzadeh, Moradinasab, and Elyasi (2017) introduced an enhanced genetic algorithm that was based on nearest neighbor search, while Smith and Imeson (2017) developed a competitive large neighborhood search heuristic for hard-instance and nonclustered problems. Mahmoudinazlou and Kwon (2024) proposed a hybrid genetic algorithm for the m-TSP to shorten the longest tour length. In addressing the TPP, strategies such as tabu search (El-Dean, 2008; Mansini, Pelizzari, & Saccomandi, 2005), simulated annealing (Voß, 1996), and genetic algorithms (Almeida, Gonçalves, Goldbarg, Goldbarg, & Delgado, 2012; Goldbarg, Bagi, & Goldbarg, 2009) have been utilized. Roy, Maity, and Moon (2023) studied a multivehicle clustered TPP with a variable-length genetic algorithm to minimize system costs by optimizing cluster selection, market visits, procurement quantities, and routing. For the family TSP, Bernardino and Paias (2021) applied population-based heuristics combined with local search methods. An overview of exact and heuristic algorithms for TPP variants is given by Manerba et al. (2017); they highlight the diverse solution approaches in the field.

2.2 Multimodal transportation

The use of different modes of transportation, such as ships, trains or trucks, can lead to a trade-off between transit time and cost. Every combination is possible in theory, but only some of the possible combinations are common in logistics systems of multimodal transport, such as truck/vessel-train-truck and truck/vessel-ship-truck, depending on the leg considered in the supply chain. ViaDonau (2012) introduced loading units to accelerate unloading processes that occur in multimodal transportation networks. Currently, there are standardized load units such as containers, swap bodies, and semi-trailers. When transshipping from inland waterways to trucks, for example, products are transferred to containers (Ghiani, Laporte, & Musmanno, 2004).

In recent studies, researchers have combined trucks and drones in multimodal models (Jeong, Song, & Lee, 2019). An example of a truck-air model is a multimodal hub location and hub network design problem, such as that developed by Alumur, Kara, and Karasan (2012). SteadieSeifi, Dellaert, Nuijten, Van Woensel, and Raoufi (2014) mentioned the different definitions of terminologies that circulate in the literature, such as multimodal, intermodal, comodal, and, more recently, synchromodal transportation. After revising these definitions, we refer to this model as a multimodal transportation model. Infante, Paletta, and Vocaturo (2009) developed a ship-truck TPP where the aim is to define the sequence with a focus on where trucks should

distribute goods to final warehouses. Sun, Hrušovskỳ, Zhang, and Lang (2018) proposed a biobjective nonlinear truck–rail routing model that minimizes the total cost and total CO2 emitted. In contrast to their work, our linear model does not require specific service sets for each mode of transportation because mode exchange can occur at any node. Fazayeli, Eydi, and Kamalabadi (2018) developed a multimodal routing-location model in which mode changes are allowed at predefined nodes. Again, the model presented in this manuscript optimizes transshipment locations and does not require specifying transshipment locations, unlike their work.

Hao and Yue (2016) used dynamic programming to solve a multimodal transportation model. They did not consider the quantities transported in their model. Instead, they assumed that the same model delivers all the quantities. Compared to their model, our model considers the number of vehicles, delivery quantity, and possibility of delivery via two modes to the same node. Zhang et al. (2011) solved a multimodal uncapacitated routing problem. The model selected one mode for each city pair. However, it did not consider the transport quantities or the possibility of having multiple vehicles with different capacities. Xiong and Wang (2014) studied a biobjective multimodal routing problem with a time window. The model minimizes the total transportation cost and total traveling time. However, they do not consider the capacity of each transportation mode. They integrated the k-shortest path and a genetic algorithm to address this problem. Moccia, Cordeau, Laporte, Ropke, and Valentini (2011) studied the multimodal routing problem with shipment consolidation options and time windows. Zameni and Razmi (2015) proposed an uncapacitated mixed-integer multimodal hub location-routing problem with simultaneous pickups and deliveries. The proposed model allocates a transportation mode to each route between the hubs and minimizes the total network cost. Riessen, Negenborn, Dekker, and Lodewijks (2015) considered barge and rail transportation modes in the container transportation problem in northwest Europe. In their model, they did consider the penalty for overdue deliveries. Demir et al. (2016) developed an intermodal service network design problem that reduces costs and emissions while using inland waterway transportation, rail, and trucks. Assadipour, Ke, and Verma (2016) proposed a bilevel biobjective mathematical model to regulate hazmat shipments by using road and rail transportation modes. The model was solved by using a particle swarm algorithm. Qu, Bektaş, and Bennell (2016) considered emission and transfer costs in service network design in a multimodal transportation problem. Tawfik and Limbourg (2019) proposed a bilevel path-based intermodal mathematical model that maximizes profit and minimizes disutility. Z. Wang and Qi (2019) studied the design of a time-dependent service network with multiple service types.

More recently, Nitsenko et al. (2020) studied the risks of multimodal transportation by using fuzzy logic. Kaewfak, Ammarapala, and Huynh (2021) developed a decision support model to determine optimal multimodal routes. The proposed multiobjective model considered transportation costs, transportation time, and seven transportation risks to improve logistics and transportation performance. In addition, the analytic hierarchy process and zero-one goal programming methods were used to determine multimodal route selection. He, Navneet, van Dam, and Van Mieghem (2021) proposed an approach to a multimodal network model and robustness assessment for

freight transport networks. They analyzed the interdependencies between transport modes and considered the disruptions of single nodes. The robustness of the network was considered based on the travel time resulting from perturbations in the network. Their model helps to schedule maintenance operations by prioritizing the critical elements in the network. The approach differs based on the proposed algorithm and the multiobjective functions. Przystupa et al. (2021) developed a multiobjective optimization model to solve a multicriteria transport problem. Their algorithm is for large-data case studies with any number of types of transport and optimization criteria. The case study considered minimizes the transportation costs and transportation risk levels. Real, Contreras, Cordeau, de Camargo, and de Miranda (2021) proposed a mixed integer programming model to solve multimodal hub design problems with flexible routes, and they developed metaheuristics based on an adaptive large neighborhood search. Ye, Jiang, Chen, Liu, and Guo (2021) proposed a bilevel mathematical model to determine the transfer location and the infrastructure capacity for a multimodal transportation network design with elastic demand. Readers may refer to Elbert, Müller, and Rentschler (2020) for a systematic review of the topic. To the best of our knowledge, none of the models in the reviewed literature optimize the selection of the transshipment port in a capacity-constrained linear problem formulation. In addition, we formulated a biobjective model by using the EcoTransit emission calculator, applied the model to a real case study, and analyzed the effect of infrastructure failure on the multimodal formulation. Real-life analysis allows for a better understanding of the optimization problem, as well as more insightful results.

3 Methodology

Our main target is to optimally determine the transportation mode and the route by considering both the total cost and the emissions. Additionally, we study the impact of considering different modes on the total cost and emissions. To achieve these goals, we compared three transportation modes, namely, inland waterway transportation, trucks, and multimodal transportation (Figure 1). The multimodal mode allows switching from one mode to another, where quantities are unloaded at a transshipment port and loaded in another mode. We consider the scenario of delivering chemical products from a depot to different ports by using three transportation modes. We list all the sets, parameters, and decision variables in Section 3.1. Then, we describe the problem, and we present the modeling concept in Section 3.2. The cost and emission calculations required for the objective function formulation are presented in Sections 3.3 and 3.4. Finally, we present the biobjective model and its solution approach in Sections 3.5 and 3.6, respectively.

3.1 Notations

The sets used are as follows:

- L: Set of ports included in the network indexed by i and j. The indices i_0, i_1 and $i_{1'}$ represent the virtual, actual and duplicated actual depots, respectively.
- M: Set of transportation modes indexed by m.

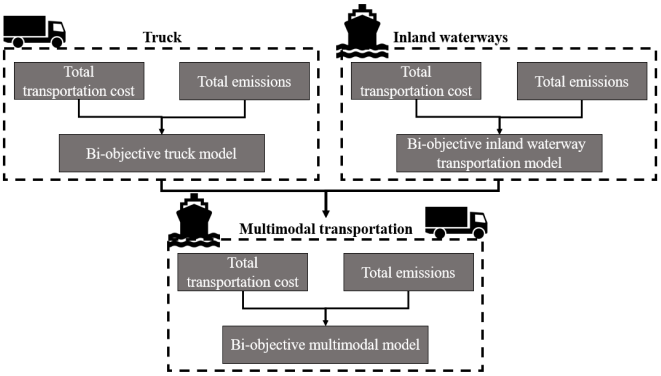

Fig. 1: The considered transportation modes and objectives

- K_m: Set of vehicles belonging to transportation mode m, indexed by k.

Table 1 lists the vehicle parameters used; they were classified as inland waterway transportation and trucks. In addition, we have:

- D_i: Demand at port i [t/day].
- S is a small number.

The decision variables for the optimization model defined in Section 3.5 are:

- $y_i^{k,m}$: Decision variable that equals 1 if port i is visited by vehicle k of mode m.
- $X_{i,j}^{k,m}$: Decision variable that equals 1 if vehicle k of mode m travels from port i to j by using vehicle k of mode m.
- $Q_i^{k,m}$: Quantity for port i loaded at vehicle k of mode m.
- $u_i^{k,m}$: Integer variable representing the sequencing of visits for port i and vehicle k of mode m.
- $f_{i,j}^{k,m}$: Continuous (nonnegative) variable that gives the total quantity loaded in vehicle k of mode m from i to j.
- $UQ_i^{k.m}$: Transshipment quantities or transfer cargo unloaded at port i by using vehicle k in mode m. These quantities are then transported by another vehicle(s) and mode m' to other ports.
- $T_i^{k,m}$: Decision variable (binary) equals 1 if vehicle k of mode m is used to transport quantities from transshipment port i.

3.2 Problem description and modeling idea

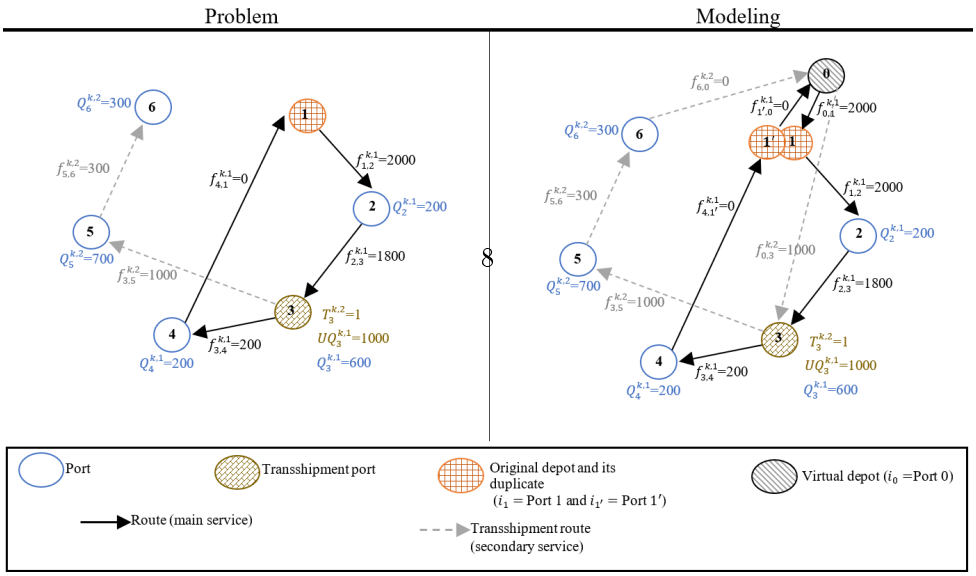

Fig. 2: Multimodal problem and modeling representation

Table 1: Description of the parameters for the various transportation modes

Notation	Description	Unit	Inland Waterway transportation	Truck
$\alpha^{k,m}$	Vehicle unit cost to cover maintenance and depreciation	[€/h]†, [€/km]††	x	x
$\beta^{k,m}$	Hourly personnel cost per worker	[€/h]	x	x
$\mu^{k,m}$	Unit fuel cost	[€/km]	x	x
p	Port charges paid by inland waterways upon unloading	[€/t]	x	
$\gamma^{k,m}$	Cost of handling transshipment (cost of loading cargo at another vehicle when changing the transportation mode)	[€/t]	x	x
$\epsilon^{k,m}$	Cost of handling deliveries (unloading costs at destination port)	[€/t]	x	x
$\Pi^{k,m}$	Rent cost for container	[€/h]		x
$\urcorner^{k,m}$	hourly truck fixed cost to cover insurance, parking and capital return	[€/h]		x
$\mathbb{T}^{k,m}$	Toll rate on highways	[€/km]		x
$n^{k,m}$	Number of workers needed to operate the vehicle	–	x*	
$d_{i,j}^{k,m}$	Distance between ports i and j using transportation mode m of vehicle$k$	[km]	x	x
$q_{i,j}$	Number of locks between ports i and$j$	–	x	
h	Docking time at the ports	[h]	x	
τ	Lock time at the locks	[h]	x	
$C^{k,m}$	Capacity of transportation mode m of vehicle$k$	[t]	x	x
η	Handling performance of port during loading and unloading activities	[t/h]	x	
$s^{k,m}$	Speed of transportation mode	[km/h]	x	x
$\kappa_{i,j}^{k,m}$	Empty percentage factor for transportation mode	–	x	x
z	conversion factor from MJ to kWh		x	
$r^{k,m}$	Load factor (utilization of transport mode)	–	x	x
ρ	Energy factor (tank-to-wheel)	[g/MJ]	x	x
ϕ	Combustion factors for NO_x, NMHC, and PM	[g/km]	x	x
ξ	Energy related emission factor (well-to-tank)	[g/MJ]	x	x
$\omega^{k,m}$	Power of transportation mode	[kW]	x	
$\chi^{k,m}$	Additional transshipment emissions resulting from material loading on vehicle k of transportation mode$m$	[g]	x	x
$E^{k,m}$	Final energy consumption	[MJ/km]		x

† : For inland waterway transportation only.

†† : For trucks only.

* : This number differs based on the barge size. The standard uses one truck worker and adds 20% buffer time to the journey. Thus, $n^{k,m}$ is not used in the truck formula.

Goods are to be transported from a depot port (i_1 = Port 1, as shown in Figure 2) to other ports by using inland waterway transportation, trucks, or both modes to fulfill the demand at each port i. Trucks are available at all ports. Thus, they can be

used for either the main service of transporting goods from the depot to other ports or the secondary service of transporting goods from a transshipment port to other ports. Figure 2 shows one main service starting from the depot (Port 1), represented by solid arrows, and visiting Ports 2, 3 and 4, after which it returns to the depot. Figure 2 also shows one secondary service (transshipment) denoted by dashed arrows starting from Port 3 and visiting Ports 5 and 6. Because inland waterway transportation is only available at the depot port, it can be used only for the main service. All vehicles starting from the depot are required to return due to capacity restrictions of the remaining ports, whereas this condition is not necessary for trucks used in the secondary service. The secondary service starting location can be any port within the main service (e.g., Ports 2, 3 or 4 in the service presented in Figure 2) where inland waterway transportation unloads additional quantities, $UQ_i^{k,m}$. These quantities are not used to satisfy the demand of the unloading port; instead, they are transported by trucks to other ports. These quantities are called transshipment quantities or transfer cargo. In Figure 2, Port 3 represents a transshipment port and receives from the main service a total of 1600 units split into two parts: $Q_3^{k,1} = 600$ to fulfill its demand and $UQ_3^{k,1} = 1000$ as transshipment to fulfill the demand of other port(s). These transshipment quantities indicate that a secondary service is used to deliver them to their final destination(s). In the proposed formulation, we model a virtual depot, i_0 =Port 0, that has a zero distance to and from all ports. This virtual depot (Figure 2) keeps the mathematical formulation simple and helps avoid complicating the subtour elimination constraints of the traveling salesman problem, as all vehicles start from and return to this virtual depot. Since trucks may start from any port if they are used in a secondary service (for transshipment), using a virtual depot means that the second port in the model solution reflects the starting port of the trucks (that is, the virtual port is ignored in translating the solution). Any vehicle performing the main service is forced to visit the original depot (i_1) from the virtual depot (i_0). However, adding the virtual depot (i_0) means that vehicles return to the virtual depot and not to the original depot (i.e., they stop at the last visited port before the virtual depot). The concept of incorporating a virtual depot has been used previously in modeling. For instance, J. Liu, Mirchandani, and Zhou (2020) introduced a virtual depot to eliminate the need for all vehicles to return to the original depot. They adopted a similar methodology in which they assumed a travel cost of 0 from all drop-off locations to the virtual depot. Annouch, Bellabdaoui, and Minkhar (2016) used a virtual depot in their open vehicle routing problem.

A duplicate of the original depot ($i_{1'}$= Port 1') is created and forced into the network such that if and only if a vehicle moves from the virtual depot to the original depot ($i_0 \rightarrow i_1$) should it also go from the duplicate original depot back to the virtual depot ($i_{1'} \rightarrow i_0$). This port modification allows the main service vehicle to return to the original depot after unloading the transshipment, and such a modification allows the secondary service vehicle to continue the delivery and to stop at the last visited port. In this configuration, a vehicle assigned to perform the main service delivers $Q_i^{k,m}$ to port i and may additionally unload the remaining carried quantities $UQ_i^{k,m}$. If $UQ_i^{k,m}$ is unloaded (i.e., $UQ_i^{k,m} > 0$), then the model deploys vehicle(s) from the virtual depot to port i (equivalent to starting a service directly from port i). The

deployed vehicle(s) can load $UQ_i^{k,m}$ and distribute it to the remaining ports in service (Figure 2). Thus, in Figure 2, the main service starting from Port 0, "virtual", and going immediately to Port 1 means that it actually starts from Port 1, and upon its return, it goes to Port 1' and ends at Port 0, which means that it actually stops at the depot (Port 1). The transshipment route (secondary service) in the figure starts from Port 0 "virtual" to Ports 3, 5 and 6, which means that the truck actually starts from Port 3, carrying the 1000 units in UQ that were unloaded by the main service and delivering them to Port 5 ($Q_5^{k,2} = 700$) and Port 6 ($Q_6^{k,2} = 300$). Let us note that in our model, the transshipment port is selected by the model and that the service mainly includes several main and several secondary services.

3.3 Cost calculations

In this section, we present the cost functions for each transportation mode. In the literature, various approaches for calculating the costs of different modes of transportation can be found. Cheng (2012) developed a model with comparable parameters, including the transshipment cost, speed, and loading capacity of the vehicles. The cost functions differ, among other factors, in their treatment of various cost elements based on regional variations. Zgonc, Tekavčič, and Jakšič (2019) introduced a regression function based on the distance between two locations. They proposed three distinct cost functions tailored for road-only, rail-only, and road-rail combined transport. Notably, for rail transport, the authors assumed that only 65% of truck costs are applicable. Janic (2007) introduced a formula for calculating the full costs associated with intermodal transport, including both internal and external factors. The internal costs within this model account for transport, time, and handling expenses; external costs are determined by factors such as demand, load factor, vehicle capacity, and an external cost factor per frequency. In this model, a cost function is not incorporated for inland waterway transportation. The transportation costs in this manuscript are based on a model of the German Federal Ministry of Transport and Digital Infrastructure, called "Bundesverkehrswegeplan 2015." The federal model is a suggestion for determining comprehensive transportation costs for various modes of transportation based on scientific understanding, as well as specific studies and interviews with industry experts (Federal Ministry of Transport and Digital Infrastructure, 2016). These cost functions are objective functions that are minimized in the model.

3.3.1 Inland Waterway Transportation

We used the transportation cost model described in the "Bundesverkehrswegeplan 2015" (Federal Ministry of Transport and Digital Infrastructure, 2016) for every transportation mode. In the cost model, transport time is defined as the sum of travel time, lock time, docking time, and handling time. The equation calculates the travel time as a cost factor. Furthermore, the equation already includes the fuel and handling costs; therefore, they do not have to be calculated.

The total distance-related cost is

$$\sum_{i\in L}\sum_{j\in L}\sum_{m\in M}\sum_{k\in K_m}(\alpha^{k,m}+\beta^{k,m}\times n^{k,m})\times\left(\frac{d_{i,j}^{k,m}}{s^{k,m}}+q_{i,j}\times\tau\right)\times X_{i,j}^{k,m}. \tag{1}$$

The total docking-related cost is

$$\sum_{i\in L}\sum_{m\in M}\sum_{k\in K_m}h\times(\alpha^{k,m}+\beta^{k,m}\times n^{k,m})\times y_i^{k,m}. \tag{2}$$

The total freight quantity-related cost is

$$\sum_{i\in L}\sum_{j\in L}\sum_{m\in M}\sum_{k\in K_m}\frac{\alpha^{k,m}+\beta^{k,m}\times n^{k,m}}{\eta}\times f_{i,j}^{k,m}. \tag{3}$$

The total fuel-related cost is

$$\sum_{i\in L}\sum_{j\in L}\sum_{m\in M}\sum_{k\in K_m}d_{i,j}^{k,m}\times\mu^{k,m}\times X_{i,j}^{k,m}. \tag{4}$$

The total unloading-related cost at the ports is

$$\sum_{i\in L}\sum_{m\in M}\sum_{k\in K_m}(p+\epsilon^{k,m})\times Q_i^{k,m}. \tag{5}$$

The total loading-related cost from one transportation mode to the other is

$$\sum_{i\in L}\sum_{m\in M}\sum_{k\in K_m}\gamma^{k,m}\times UQ_i^{k,m}. \tag{6}$$

The total cost of inland waterway transportation in [€] is denoted by c_s. It is given by

$$c_s=(1)+(2)+(3)+(4)+(5)+(6). \tag{7}$$

3.3.2 Trucks

The following transportation cost model was proposed by Federal Ministry of Transport and Digital Infrastructure (2016). We have added the handling costs for unloading freight based on expert knowledge.

The total transportation-related cost is

$$\sum_{i\in L}\sum_{j\in L}\sum_{m\in M}\sum_{k\in K_m}X_{i,j}^{k,m}\times\frac{1}{1-\kappa_{i,j}^{k,m}}\times\left[d_{i,j}^{k,m}\times(\mu^{k,m}+\alpha^{k,m})+\left(\frac{d_{i,j}^{k,m}}{s^{k,m}}\times 1.2+2\right)\times\right. \tag{8}$$

$$\left.(\beta^{k,m}+\Pi^{k,m})+\frac{d_{i,j}^{k,m}}{s^{k,m}}\times 1.2\times\urcorner^{k,m}+\mathbb{T}^{k,m}\times d_{i,j}^{k,m}\right].$$

The total unloading-related cost at the port is

$$\sum_{i \in L} \sum_{m \in M} \sum_{k \in K_m} \epsilon^{k,m} \times Q_i^{k,m}. \tag{9}$$

The total loading-related cost from one transportation mode to the other is

$$\sum_{i \in L} \sum_{m \in M} \sum_{k \in K_m} \gamma^{k,m} \times UQ_i^{k,m}. \tag{10}$$

The total cost of trucks in [€] is denoted as c_t. It is given by

$$c_t = (8) + (9) + (10). \tag{11}$$

3.4 Emission calculations

In the following section, we present the functions used to calculate the gas emissions. The model calculates energy consumption based on distance. We identify the methodology of EcoTransit (Institut für Energie- und Umweltforschung Heidelberg gGmbH, 2023) as the most well-documented; it offers the possibility of transferring it to multimodal transportation because it calculates different emissions such as CO_2 emissions, CO_2 equivalents, greenhouse gases, and energy consumption for trucks, rail, maritime transportation, and inland waterway transportation. The well-to-wheel (WTW) emissions are more comparable among the different transportation modes. The WTW includes energy consumption and production, and emissions are calculated for different legs, which means that the emissions are between two ports by one transportation mode. This tool allows for the calculation of greenhouse gas emissions, energy consumption, and CO_2 emissions. This norm includes two methods: consumption-based and distance-based methods. EcoTransit uses a general methodology for the various transportation modes. Because energy consumption and greenhouse gas emissions are both affected by similar factors, we decided to focus on only one of them in terms of emissions. Finally, this model was used to calculate greenhouse gas emissions (Institut für Energie- und Umweltforschung Heidelberg gGmbH, 2023).

3.4.1 Inland Waterway Transportation

The transportation-related emissions are

$$\sum_{i \in L} \sum_{j \in L} \sum_{m \in M} \sum_{k \in K_m} X_{i,j}^{k,m} \times d_{i,j}^{k,m} \times (1 + \kappa_{i,j}^{k,m}) \times \left(\frac{\omega^{k,m}}{s^{k,m}} \times z \times (\rho + \xi) + \phi_{\mathrm{NO_x}} + \phi_{\mathrm{NMHC}} + \phi_{\mathrm{PM}}\right). \tag{12}$$

The transshipment-related emissions are

$$\sum_{i \in L} \sum_{m \in M} \sum_{k \in K_m} \chi^{k,m} \times UQ_i^{k,m}. \tag{13}$$

The total quantity of emissions from inland waterway transportation in $[g]$ is denoted by e_s. It is given by

$$e_s = (12) + (13). \tag{14}$$

3.4.2 Trucks

The transportation-related emissions are

$$\sum_{i\in L}\sum_{j\in L}\sum_{m\in M}\sum_{k\in K_m}\frac{d_{i,j}^{k,m}}{1+\kappa_{i,j}^{k,m}}\times(E^{k,m}\times(\rho+\xi)+\phi_{\mathrm{NO_x}}+\phi_{\mathrm{NMHC}}+\phi_{\mathrm{PM}})\times X_{i,j}^{k,m}. \tag{15}$$

The transshipment-related emissions are

$$\sum_{i\in L}\sum_{m\in M}\sum_{k\in K_m}\chi^{k,m}\times UQ_i^{k,m}. \tag{16}$$

The total quantity of emissions from trucks in $[g]$ is denoted by e_t. It is given by

$$e_t = (15) + (16). \tag{17}$$

3.5 Biobjective optimization problem

Based on the above notation and definitions, we formulate a biobjective optimization problem. The total cost and quantity of emissions are denoted by c and e, respectively. The model objective functions are as follows:

$$\min c = c_s + c_t, \tag{18}$$

$$\min e = e_s + e_t. \tag{19}$$

The model is subject to the following constraints.

$$\sum_{j\in L}X_{i,j}^{k,m}=\sum_{j\in L}X_{j,i}^{k,m},\quad \forall i\in L,\quad \forall k\in K_m,\quad \forall m\in M, \tag{20}$$

$$y_i^{k,m}=\sum_{j\in L}X_{i,j}^{k,m},\quad \forall i\in L,\quad \forall k\in K_m,\quad \forall m\in M, \tag{21}$$

$$\sum_{k\in K_m}\sum_{j\in L}X_{i_0,j}^{k,m}\le|K_m|,\quad \forall m\in M, \tag{22}$$

$$S\times y_i^{k,m}\le Q_i^{k,m}+T_i^{k,m}\le D_i\times y_i^{k,m},\quad \forall i\in L\setminus\{i_0,i_1,i_{1'}\},\quad \forall k\in K_m,\quad \forall m\in M, \tag{23}$$

$$Q_i^{k,m}\le C^{k,m}\times(1-T_i^{k,m}),\quad \forall k\in K_m,\quad \forall m\in M,\quad \forall i\in L\setminus\{i_0,i_1,i_{1'}\}, \tag{24}$$

$$u_i^{k,m} - u_j^{k,m} + C^{k,m} \times X_{i,j}^{k,m} \leq C^{k,m} - Q_i^{k,m}, \quad \forall k \in K_m, \\ \forall m \in M, \forall i, j \in L \setminus \{i_0\} : i \neq j : D_i + D_j \leq C^{k,m}, \tag{25}$$

$$Q_i^{k,m} \leq u_i^{k,m} \leq C^{k,m}, \quad \forall i \in L \setminus \{i_0\}, \quad \forall k \in K_m, \quad \forall m \in M, \tag{26}$$

$$\sum_{j \in L \setminus \{i\}} f_{i,j}^{k,m} = \sum_{j \in L \setminus \{i\}} f_{j,i}^{k,m} - Q_i^{k,m} - UQ_i^{k,m}, \quad \forall i \in L \setminus \{i_0, i_1, i_{1'}\}, \quad \forall k \in K_m \quad \forall m \in M, \tag{27}$$

$$\sum_{j \in L \setminus \{i_0\}} f_{i_0,j}^{k,m} = \sum_{j \in L \setminus \{i_0\}} Q_j^{k,m} + UQ_j^{k,m}, \quad \forall k \in K_m, \quad \forall m \in M, \tag{28}$$

$$f_{i,j}^{k,m} \leq C^{k,m} \times X_{i,j}^{k,m}, \quad \forall i \in L, \quad \forall j \in L, \quad \forall k \in K_m, \quad \forall m \in M, \tag{29}$$

$$\sum_{m \in M} \sum_{k \in K_m} Q_i^{k,m} = D_i, \quad \forall i \in L, \tag{30}$$

$$\sum_{i \in L} Q_i^{k,m} + \sum_{i \in L} UQ_i^{k,m} \leq C^{k,m} \times \sum_{i \in L \setminus \{i_0\}} X_{i_0 i}^{k,m}, \quad \forall k \in K_m, \quad \forall m \in M, \tag{31}$$

$$X_{i_0,j}^{k,m} = T_j^{k,m}, \quad \forall j \in L \setminus \{i_0, i_1, i_{1'}\}, \quad \forall k \in K_m, \quad \forall m \in M, \tag{32}$$

$$X_{i_0,i_1}^{k,m} + \sum_{i \in L \setminus \{i_0,i_1\}} T_i^{k,m} = y_{i_0}^{k,m}, \quad \forall k \in K_m, \quad \forall m \in M, \tag{33}$$

$$\sum_{i \in L} Q_i^{k,m} \leq \sum_{m' \in M : m' \neq m} \sum_{k' \in K_m : k' \neq k} UQ_j^{k',m'} + C^{k,m} \times (1 - T_j^{k,m}), \\ \forall k \in K_m, \quad \forall m \in M, \quad \forall j \in L \setminus \{i_0, i_1, i_{1'}\}, \tag{34}$$

$$\sum_{i \in L} UQ_i^{k,m} \leq C^{k,m} \times X_{i_0,i_1}^{k,m}, \quad \forall k \in K_m, \quad \forall m \in M, \tag{35}$$

$$\sum_{k \in K_m} UQ_i^{k,m} \leq \sum_{m' \in M} \sum_{k' \in K_m} C^{k',m'} \times T_i^{k',m'}, \quad \forall i \in L \setminus \{i_0, i_1, i_{1'}\}, \quad \forall m \in M, \tag{36}$$

$$\sum_{m \in M} \sum_{k \in K_m} f_{i_0,i}^{k,m} = \sum_{m \in M} \sum_{k \in K_m} UQ_i^{k,m}, \quad \forall i \in L \setminus \{i_0, i_1, i_{1'}\}, \tag{37}$$

$$\sum_{i \in L \setminus \{i_0, i_1\}} f_{i_0,i}^{k,m} \geq S \times \sum_{i \in L \setminus \{i_0, i_1\}} T_i^{k,m}, \quad \forall k \in K_m, \quad \forall m \in M, \tag{38}$$

$$f_{i_0,i_1}^{k,m} \geq S \times y_{i_1}^{k,m}, \quad \forall k \in K_m, \quad \forall m \in M, \tag{39}$$

$$X_{i_0,i_1}^{k,m} = X_{i_{1'},i_0}^{k,m}, \quad \forall k \in K_m, \quad \forall m \in M, \tag{40}$$

$$\begin{aligned} &T_i^{k,m} = 0, \quad \forall i \in \{i_0, i_1, i_{1'}\}, \forall k \in K_m, \quad \forall m \in M, \\ &UQ_i^{k,m} = 0, \quad \forall i \in \{i_0, i_1, i_{1'}\}, \forall k \in K_m, \quad \forall m \in M. \end{aligned} \tag{41}$$

Constraint (20) ensures that if vehicle k of mode m enters a port, it exits. Constraint (21) links $y_i^{k,m}$ with $X_{i,j}^{k,m}$ such that if a port is not visited, its arcs are not used. Constraint (22) ensures that the maximum number of available vehicles is not exceeded in each mode. Constraint (23) links $y_i^{k,m}$ with $Q_i^{k,m}$ such that if no quantity is delivered, then $y_i^{k,m}$ is 0. The exceptions are virtual and actual depots. In this constraint, we further link the virtual depot and transshipment port such that if port i is used, then $T_i^{k,m}$ and $y_i^{k,m}$ are 1 with no quantity delivered. Constraint (24) ensures that if there is a transshipment at port i, the vehicle that starts from this port to deliver to other ports does not include a delivery to this port. Constraints (25) and (26) are Miller–Trucker–Zemlin (MTZ) subtour elimination constraints that ensure that a vehicle does not subtour on a route. Constraint (27) defines the flow from i to j as the flow that enters i from all possible j values minus the quantities. Constraint (28) defines the first flow as the total loaded quantity. Constraint (29) links $f_{i,j}^{k,m}$ with $X_{i,j}^{k,m}$ so that $f_{i,j}^{k,m}$ is zero if the corresponding $X_{i,j}^{k,m}$ is zero. Constraint (30) ensures that the total quantity unloaded by multiple vehicles at one port is equal to the demand. Constraint (31) ensures that the total delivered and unloaded quantities of vehicle k in mode m do not exceed the vehicle capacity if the vehicle is used. Constraint (32) links $T_j^{k,m}$ with $X_{i,j}^{k,m}$ such that if $T_j^{k,m} = 1$, the vehicle moves directly from the virtual depot to the transshipment port j. Constraint (33) states that if vehicle k of transportation mode m is used from the virtual depot, the vehicle must either use the arc from the virtual depot to the actual depot or be used at a transshipment port.

Constraint (34) ensures that the quantity delivered to the ports from transshipment port j does not exceed the total quantity unloaded by other vehicles from other modes at port j. Constraint (35) ensures that unloaded quantities are allowed if and only if the vehicle moves from the virtual depot to the actual depot (i.e., the vehicle starts from the actual depot). Constraint (36) ensures that the number of vehicles and their capacities are sufficient to transport the unloaded quantity at port i. Constraint (37) ensures that all the unloaded quantities are delivered. Constraint (38) ensures that if a vehicle is used at the exchange port, then it must deliver some quantities; that is, the initial flow should be positive. Constraint (39) states that the vehicle must carry some nonzero quantities if it travels from the virtual port to the actual port. Constraint (40) ensures that if a vehicle moves from the virtual depot to the original

depot, it moves from the original depot to the virtual depot. Consequently, the tour is complete. Constraint (41) prevents unloading at the actual and virtual depots. Section B of the Appendix shows the steps required to convert the multimodal model into a single-mode model.

3.6 Biobjective optimization approach

Dealing simultaneously with cost minimization and emission reduction leads to a biobjective optimization with two conflicting goals. Improving cost efficiency may worsen emissions and vice versa. For instance, in inland waterway transportation, prioritizing cost minimization might emphasize total docking and freight-related costs over total distance and fuel costs. This approach can result in better cost performance but can produce higher emissions due to a slight increase in fuel consumption and distance traveled. Conversely, focusing on emission reduction tends to reduce travel distance and, consequently, fuel consumption, leading to lower emissions while inducing higher costs associated with docking and freight handling. Several studies in the literature have explored these conflicting costs and emission objectives across different modes of transportation, such as ground transportation (Cheaitou, Hamdan, Larbi, & Alsyouf, 2021; Demir et al., 2016; Molina, Eguia, Racero, & Guerrero, 2014) and maritime transportation (Dulebenets, 2018; Zhao, Fan, Zhou, & Kuang, 2019). As a result, there is a set of nondominated, efficient, optimal solutions that are Pareto-optimal (Fonseca & Fleming, 1998). Pareto points can be obtained by using several methods, such as the utility function method, lexicographic method, goal programming, normal boundary intersection method and evolutionary algorithms (Ghane-Kanafi & Khorram, 2015; Singh & Yadav, 2023). The method choice depends on the preference availability from decision-makers (no preference method, a priori, a posteriori and interactive methods). In this work, an a priori scalarization method is used because the decision-maker preference is known in advance. The weighted comprehensive criterion method is used to solve the biobjective problem because of its simplicity and suitability for heuristics because it does not introduce additional constraints.

In this method, the multiobjective function must be divided into two single functions that dispose of different units and orders of magnitude. On the one hand, the cost function is in €, and on the other hand, the emission function is in g. Single objective functions are defined as objective functions and are subject to the same constraints in the respective sections. Both single subproblems are solved to obtain the optimal solutions, which we call $c_{\min}$ and $e_{\min}$. After receiving both single optimal solutions, we merge them into a single normalized objective function (Dehghani, Esmaeilian, & Tavakkoli-Moghaddam, 2013). The equations used to normalize the objective functions are as follows:

$$c' = \frac{c - c_{min}}{c_{min}}, \tag{42}$$

$$e' = \frac{e - e_{min}}{e_{min}}. \tag{43}$$

Equations (42) and (43) are the relative variations between the single objective functions of the transportation costs and emission costs and their respective optimal values. We then multiply each normalized single-objective function by a relative weight, depending on the decision-maker. This multiplication leads to the following objective function.

$$\min \delta = a_1 \times c' + a_2 \times e', \tag{44}$$

where a_1 and a_2 are the weights that depend on the decision-maker, and $a_1 + a_2 = 1$. This objective function is minimized and is subject to the same constraints as the initial problem. For a given set of a_1 and a_2, there is only one Pareto-optimal solution. However, if these weights are changed, different Pareto-optimal solutions may result (Marler & Arora, 2004). The use of the scalarization technique may not result in all Pareto optimal points, as this depends on convexity, among other factors (Ghane-Kanafi & Khorram, 2015).

4 Solution approach

This problem is a generalization of the traveling purchaser problem, which is an *NP*-hard problem (see Section A in the appendix). Therefore, the problem cannot be solved by using an exact approach for large instances. We use a population-based heuristic to overcome this issue by designing search operators to align with the studied problem. An interesting advantage of population-based heuristics is the possibility of adapting them through the design of search operators, number of iterations and population size to control solution quality and computation time. Population-based heuristics have been used successfully in the literature to solve similar problems, such as TSP with processing time (Bożejko & Wodecki, 2009), heterogeneous VRP (S. Liu, 2013), TPP with speed optimization (Cheaitou, Hamdan, Larbi, & Alsyouf, 2021), dynamic VRP with unknown customers (Créput, Hajjam, Koukam, & Kuhn, 2012; Sabar, Goh, Turky, & Kendall, 2021), capacitated electric VRP (C. Wang, Qin, Xiang, Jiang, & Zhang, 2023), periodic VRP (Borthen, Loennechen, Wang, Fagerholt, & Vidal, 2018; Vidal, Crainic, Gendreau, Lahrichi, & Rei, 2012) and liner shipping (Cariou, Cheaitou, Larbi, & Hamdan, 2018; Cheaitou, Hamdan, & Larbi, 2021). In addition, variants of this heuristic have been successfully used in other domains, such as supplier selection (Hamdan, Cheaitou, Shikhli, & Alsyouf, 2023), maintenance strategy optimization (Alsharqawi, Abu Dabous, Zayed, & Hamdan, 2021), machine scheduling (Nearchou, 2010) and aircraft motion planning (Wu, 2021).

The heuristic used to solve the problem is presented in Algorithm 1. It starts by calling a **population generation** subroutine (see Section C in the appendix) to create a population ($\mathcal{P}$) of Ψ feasible individuals (potential solutions) that should be multiples of the total number of operators ($\Omega = 18$). The randomly generated feasible individuals satisfy all the model constraints (20) – (41). The structure of each individual is detailed in Section D.1 in the appendix. The global cost, the emission, and the variation values are initialized as follows: $c_{\text{global}} = \infty$, $e_{\text{global}} = \infty$ and $\delta_{\text{global}} = \infty$. The algorithm attempts to enhance the quality of individuals in each iteration under a predefined total number of iterations or generations (G).

In each iteration, $g = 1, ..., G$, the algorithm first calculates the cost and emission objective function (c_ψ and e_ψ) by using Equations (18) and (19) for each individual (Algorithm 2). Based on the optimization setting (ObjType), either a single objective or a biobjective optimization is executed. In the case of single objective setting, the algorithm compares the best cost (emission) value for all individuals with the global cost (emission) value and updates c_{global} (e_{global}) accordingly. The algorithm returns c_{global} as the best objective value and the corresponding solution details (i.e., route sequence, quantity allocation and vehicle assignment). In addition, it returns the corresponding total emission (cost) value and updates relevant heuristic parameters, such as Ξ. In the case of the biobjective setting and before calculating the variations, the global variation is recalculated if the global cost (c_{global}) or global emissions (e_{global}) are updated. This procedure ensures the use of the most recent reference points for the variation calculation. The variation for each individual (δ_ψ) is calculated by using Equation (44). Then, the algorithm identifies the best objective function value in the current iteration ($\min_{\psi \in \{1,...,\Psi\}} \delta_\psi$) and compares it with the current global objective value δ_{global}. The algorithm then updates the global objective value if the best-found objective value is better than the current global objective value. The algorithm returns the best objective value δ_{global}, which corresponds to the solution details, the corresponding total cost and emission of the best individual and the updated heuristic parameters, such as Ξ, c_{global} and e_{global}, as shown in Algorithm 2.

Finally, the algorithm randomly divides all individuals (Ψ) into subsets, called φ_υ, each of which is Ω individuals. These subsets are constructed randomly. In each subset, the algorithm identifies and selects the best individual in terms of the value of Equation (18), (19), or (44) depending on the optimization setting (ObjType) in the subset then uses one operator at a time to produce a new individual from each operator, which results in a total of Ω individuals stored in a temporary population $\mathcal{P}_{\text{tmp}}$. The Ω operators used in the algorithm are as follows:

- *Operator 1:* Keep the best individual in the subgroup unchanged "Do nothing".

  Route operators (refer to Section D.2):
- *Operator 2:* Randomly select one vehicle and flip its route.
- *Operator 3:* Randomly select multiple vehicles then flip the route of each vehicle.
- *Operator 4:* Randomly select one vehicle and swap its route.
- *Operator 5:* Randomly select multiple vehicles then swap the route of each vehicle.
- *Operator 6:* Randomly select one vehicle and slide its route.
- *Operator 7:* Randomly select multiple vehicles then slide routes for each vehicle.

  Starting point operator (refer to Section D.3):
- *Operator 8:* Randomly select a vehicle that starts from a transshipment port and force it to start from the depot.

  Vehicle type operators (refer to Section D.4):
- *Operator 9:* Change the vehicle type of a random vehicle to a lower capacity.
- *Operator 10:* Randomly change the vehicle type of a random vehicle.

  The quantity exchange operators are as follows (refer to Section D.5):
- *Operator 11:* Randomly exchange two ports between two random vehicles.

- *Operator 12:* Conduct multiple random port exchanges between two random vehicles.
- *Operator 13:* Randomly select two vehicles then exchange unique ports with similar quantities.
- *Operator 14:* Select multiple random vehicles and exchange unique ports with similar quantities.

The quantity transfer operators are as follows (refer to Section D.6):

- *Operator 15:* Randomly transfer quantities from the vehicle with the lowest utilization to the vehicle with the highest utilization.
- *Operator 16:* Randomly transfer quantities from multiple vehicles with low utilization to the vehicle with high utilization until it is fully utilized.
- *Operator 17:* Randomly transfer quantities from one port to another between random vehicles.
- *Operator 18:* Randomly transfer quantities from multiple ports served by one random vehicle to another random vehicle.

The operators are designed such that the feasibility of the individual operator is not affected. Since the initial individuals are feasible, the operators maintain this feasibility, where any quantity movement is permitted only after ensuring that enough capacity is available (capacity is never violated in this case). In addition, since the initial chromosomes satisfy the demand requirements and none of the operators create or generate additional quantities, demand constraints are not impacted. Route and other constraints are respected through chromosome design. The algorithm then replaces all old individuals (Ψ) with newly produced individuals in the temporary population $\mathcal{P}_{\text{tmp}}$ created by the Ω operators. Notably, one of the operators performs no changes on the solution. Thus, the best individual in each subset is kept unchanged and moved to the next iteration. Moreover, the heuristic discards all individuals and produces a new generation if the number of iterations without improvement in the solution counter (Ξ) reaches a predefined limit Γ. The process continues until the maximum number of iterations (G) is reached.

5 Real-life case study

In this section, we consider the real case study of the West German canal system. The case study is used to evaluate heuristic performance in Section 6.3 and to derive the managerial insights presented in Section 7.

We examine historical goods and inland waterway transportation flows across the canal system for the research project *Preview*. We also evaluate the stake-holding industries and their expected cost impact on transport due to disruptions, such as queues at locks or unforeseen infrastructure failures. The expected cost impact on the entire supply chain is more severe because, among others, these costs include the management effort for modal shift to trucks, time-sensitive market premiums, and subsequent costs if supply chain operations are delayed. Since the infrastructure of the West German canal system is old, critical points from the logistics perspective must be identified, and the need for a multimodal split will be analyzed. Wehrle, Wiens, Schultmann, Akkermann, and Bödefeld (2020) provided more insights into

Algorithm 1 Main heuristic

Input: Context-related: (L, M, K_m, D_i), vehicle-related: ($\alpha^{k,m}$, $C^{k,m}$, $\beta^{k,m}$, $n^{k,m}$, $d_{i,j}^{k,m}$, $q_{i,j}$ h, τ, η, $\mu^{k,m}$, p, $\epsilon^{k,m}$, $\gamma^{k,m}$, $s^{k,m}$, $\Pi^{k,m}$ $\urcorner^{k,m}$, $\mathbb{T}^{k,m}$, $\kappa_{i,j}^{k,m}$, z, $r^{k,m}$, ρ, ϕ, ξ, $\omega^{k,m}$, $\chi^{k,m}$, $E^{k,m}$), and heuristic-related: (G, Ψ, Ω, Γ, ObjType).
Output: The best total cost, the best total emission, the best route for each vehicle, quantities delivered by each vehicle.
set $c_{\text{global}} \leftarrow \infty$, $e_{\text{global}} \leftarrow -\infty$, $\delta_{\text{global}} \leftarrow \infty$ and $\Xi = 0$
$\mathcal{P}$ $\leftarrow$ **Population Generation**(Context-related, vehicle-relate and heuristic-related parameters, Ψ)
for $g \leftarrow 1$ **to** G **do**
    {Best value and corresponding details, Ξ, c_{global}, e_{global}, δ_{global} } $\leftarrow$ **Get Objective Value**(Context-related, vehicle-relate and heuristic-related parameters, Ξ, c_{global}, e_{global}, δ_{global})
    divide $\mathcal{P}$ randomly and equally into Υ sub groups (φ_υ) of Ω Individuals.
    for $\upsilon \leftarrow 1$ **to** Υ **do**
        select the best individual from φ_υ:
$$\Delta = \begin{cases} \text{argmin}_{\psi \in \varphi_\upsilon} c_\psi, & \text{if ObjType} = \text{`Cost'} \\ \text{argmin}_{\psi \in \varphi_\upsilon} e_\psi, & \text{if ObjType} = \text{`Emission'} \\ \text{argmin}_{\psi \in \varphi_\upsilon} \delta_\psi, & \text{if ObjType} = \text{`Bi'} \end{cases}$$
        perform Ω operations on the best individual (φ_υ^Δ)
        store new individuals in $\mathcal{P}_{\text{tmp}}$
    end for
    if $\Xi > \Gamma$ **then**
        discard Ψ individuals in $\mathcal{P}$ and $\mathcal{P}_{\text{tmp}}$
        $\mathcal{P}$ $\leftarrow$ **Population Generation**(Context-related, vehicle-relate and heuristic-related parameters,Ψ)
    else
        $\mathcal{P} \leftarrow \mathcal{P}_{\text{tmp}}$
    end if
end for
return the heuristic best solution.

the resiliency issues of the West German canal system and noted the importance of inland waterway transportation in Germany. Their model helps to detect critical infrastructure to schedule the maintenance of the infrastructure of the system.

Figure 3 provides a detailed view of the different canals. There are four canals that belong to the West German canal system. Duisburg was the starting point for the base scenario. Inland waterway transportation must include canals. Consequently, if one port is not available, the distance from one port to the other is often greater than is the relative failure of roads because there are more alternatives for trucks in the event of any failure.

We used 16 ports and 14 locks. The water level is 1.9 meters in the baseline scenario. All locks and ports were available, and the lock time was 40 minutes. Because of the

Algorithm 2 Get objective value

Input: Context-related, vehicle-related and heuristic-related parameters, $c_{\text{global}}, e_{\text{global}}$, δ_{global}, and Ξ
Output: The best objective value and the corresponding solution details.
for $\psi \leftarrow 1$ **to** Ψ **do**
    evaluate Equations (18) and (19) and **store** the values in c_ψ and e_ψ, respectively
end for
if TypeOPT = 'Cost' **then**
    if $\min_{\psi \in \{1,\ldots,\Psi\}} c_\psi < c_{\text{global}}$ **then**
        store the solution of $(\text{argmin}_{\psi \in \{1,\ldots,\Psi\}} c_\psi)$ individual
        $\Xi \leftarrow 0$
    else
        $\Xi \leftarrow \Xi + 1$
    end if
    return the updated c_{global} and its corresponding solution details and total emission value, and the updated Ξ.
end if
if TypeOPT = 'Emission' **then**
    if $\min_{\psi \in \{1,\ldots,\Psi\}} e_\psi < e_{\text{global}}$ **then**
        store the solution of $(\text{argmin}_{\psi \in \{1,\ldots,\Psi\}} e_\psi)$ individual
        $\Xi \leftarrow 0$
    else
        $\Xi \leftarrow \Xi + 1$
    end if
    return the updated e_{global} and its corresponding solution details and total cost value, and the updated Ξ.
end if
if TypeOPT = 'Bi' **then**
    if $\min_{\psi \in \{1,\ldots,\Psi\}} c_\psi < c_{\text{global}}$ **and** $g \neq 1$ **then**
        recalculate δ_{global} using $\min_{\psi \in \{1,\ldots,\Psi\}} c_\psi$
    end if
    if $\min_{\psi \in \{1,\ldots,\Psi\}} e_\psi < e_{\text{global}}$ **and** $g \neq 1$ **then**
        recalculate δ_{global} using $\min_{\psi \in \{1,\ldots,\Psi\}} e_\psi$
    end if
    for $\psi \leftarrow 1$ **to** Ψ **do**
        evaluate Equation (44) and **store** the value in δ_ψ
    end for
    if $\min_{\psi \in \{1,\ldots,\Psi\}} \delta_\psi < \delta_{\text{global}}$ **then**
        store the solution of $(\text{argmin}_{\psi \in \{1,\ldots,\Psi\}} \delta_\psi)$ individual
        $\Xi \leftarrow 0$
    else
        $\Xi \leftarrow \Xi + 1$
    end if
    return the updated δ_{global} and its corresponding solution details, total cost and emission values, the and the updated c_{global}, e_{global} and Ξ.
end if

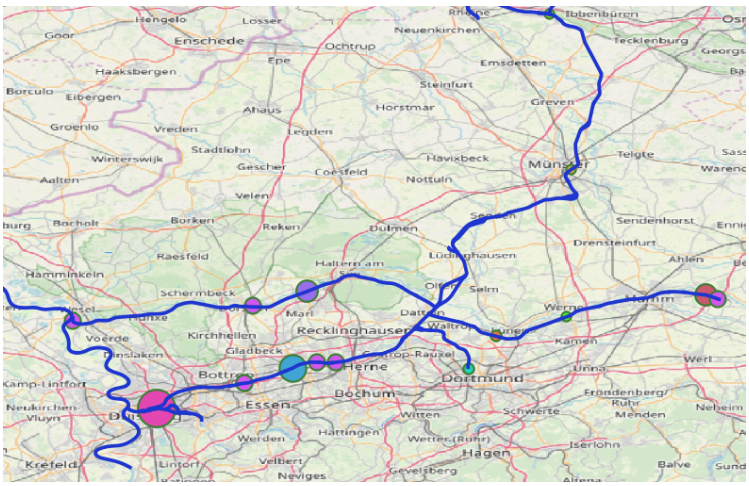

Fig. 3: Network of the West German canal system. Data: Fachserie Binnenschiffahrt. (StatistischeBundesamt, 2019) Layout: OpenStreetMap

high demand for industries in that region, we compared inland waterway transportation and a package of ten trucks in our case study as a reasonable relaxation. Effects such as platooning have not yet been considered, even though they have been evaluated in practice to reduce fuel costs and emissions. Therefore, four ships with different capacities and input parameters were included. Trucks and inland waterway transportation use diesel engines. We focused on the chemistry industry. The international standard for measuring greenhouse gas emissions, ISO14083, is the new equivalent to the German DIN EN 16258 standard for reporting and for quantifying greenhouse gas emissions from transportation operations (ISO, 2019). The demand is based on historical data of the last ten years of freight spending in canal systems and ports published in the "Fachserie Binnenschifffahrt" (StatistischeBundesamt, 2019). The distances are calculated with the Here-API and the website of Institut für Energie- und Umweltforschung Heidelberg gGmbH (2023) for inland waterways because the Here-API does not include canal navigation. In Managerial Insights 1–3, we consider situations where the decision-maker decides that the two objective functions are equally important to the project. Consequently, we set the importance weights (a_1 and a_2) to 0.5. Let us note that a decision-maker may utilize a multicriteria decision-making tool, such as the analytic hierarchy process, to assess the importance of each objective. Table 2 lists the ports and locks considered in this case study, where Duisburg is the actual depot for the model. Tables E1–E6 in Appendix E provide the data used in this study. The real-life case study provides answers to the following questions:

- What situations make the use of multimodal transportation more attractive than unimodal transportation?
- What effects do variable lock times have on the total cost?
- What are the advantages of multimodal transportation in the event of infrastructure failures?

- What is the trade-off between costs and emissions when using multimodal transportation?

Table 2: Ports and locks in the case study

Index	Port	Lock
0	Emsland	Meiderich
1	Münster	Oberhausen
2	Dortmund	Gelsenkirchen
3	Rhein-Lippe	Wanne-Eickel
4	Marl	Herne-Ost
5	Lünen	Henrichenburg
6	Bergkamen	Datteln
7	Hamm	Ahsen
8	Schmehausen	Flaesheim
9	Bottrop	Dorsten
10	Essen	Hünxe
11	Coelln-Neuessen	Friedrichsfeld
12	Ruhr Öl	Hamm
13	Gelsenkirchen	Münster
14	Wanne-Eickel	-
15	Duisburg (depot)	-

6 Numerical experiments

In this section, we study the problem complexity to understand the impact of the number of ports, the demand and the number of vehicles on the complexity of the exact solution. We also analyze the impact of heuristic parameters (maximum number of iterations G, maximum number of individuals Ψ and the number of iterations without improvement in the solution Γ) on the solution quality and time. Finally, we present the heuristic performance against the exact approach. All experiments were conducted by using a computer equipped with an Intel(R) Core(TM) i7-9750H CPU @ 2.6 GHz and 16 GB of RAM running the Windows 10 Home 64-bit operating system. Let us note that since the heuristic uses a randomized process to generate its initial population and in applying operators, we solved each instance ten times and computed the average to determine the performance and the robustness. We used CPLEX 20.1.0 to obtain the exact solution; we set a time limit of three hours as the stopping criterion for the solver.

6.1 Impact of system parameters on the exact solution complexity

This biobjective multimodal transportation problem is *NP*-hard since it can be reduced to a TSP problem, which is also proven to be *NP*-hard. We conduct a complexity study to understand the contributions of parameters to the problem complexity. We vary the number of ports $|L| = \{8, 13, 18, 23\}$. Let us note that for each problem size, the first three ports are the virtual depot, the depot and its duplicate. We also

increase the demand by a factor F_D, $F_D = \{1, 1.3, 1.5, 1.7\}$. In addition to understand the impact of vehicles, we increase the number of vehicles F_{K_m}, $F_{K_m} = \{1, 1.5, 2, 2.5\}$. Let us note that we consider the instance with $|L| = 5$, $F_D = 1$, and $F_{K_m} = 1$ as a baseline case. In each experiment, we record the exact solving time and the solver's gap, and then, we combine the two to form a complexity score (complexity score = $0.5 \times \frac{\text{Computation time}}{\text{Time limit}} + 0.5 \times \text{MIP gap}$). Let us note that in these experiments, we average the complexity score of the three objective functions (cost only, emission only and the biobjective).

A score between 0 and 0.5 means that an exact optimal solution (MIP gap = 0) is found within the time limit. A complexity score higher than 0.5 means that the time limit (computation time = time limit) is reached and that the increased part represents the MIP gap, and a score greater than 1 means that the MIP gap when the time limit is reached is greater than 100%. Figure 4 shows the complexity score under the experimental setup from the baseline case. Figure 4a shows the complexity score as a function of the demand factor and the number of ports. It is clear that increasing both the demand and the number of ports increase the complexity. However, it is difficult to say that increasing demand results in only greater complexity for a given number of ports (e.g., at $|L| = 20$, see $F_D = 1.3$ and $F_D = 1.5$). This is due to the high variability in the MIP Gap of the different instances. However, increasing the number of ports only increases the complexity (see, for instance, the different problem sizes at $F_D = 1$). Figure 4b illustrates the effect of the number of vehicles (represented by the vehicle factor, F_{K_m}) and the number of ports on the problem complexity from the baseline case. A greater number of vehicles increases the complexity score; although in some instances, the increased number of vehicles slightly reduces the complexity (see $|L| = 18$, from $F_{K_m} = 2$ to $F_{K_m} = 2.5$). Instances with more than 13 ports and high demand ($F_D \geq 1.5$) and more than 23 ports and a high number of vehicles ($F_{K_m} \geq 2$) experience high complexity and cannot be solved by using the exact approach (Figure 4, for which the score is greater than 0.5). Three-way analysis of variance (ANOVA) was used to understand the impact of the three parameters. The test results indicate that the number of ports only and the number of vehicles only have significant impacts on the complexity score (p values = 0 and 0.002, respectively), while the demand factor does not have a statistically significant impact on the complexity score (p value = 0.1771). In addition, the combination of both the number of ports and the number of vehicles and the combination of demand and number of vehicles and the combination of all three factors were found to have a statistically significant impact on the complexity score (p values = 0.007, 0 and 0, respectively).

6.2 Impact of heuristic parameters

We generated 21 instances with different characteristics to analyze the impact of heuristic parameters on the solution quality and time of the multimodal model. Table 3 shows the characteristics of these instances. In the following experiments, we varied the number of iterations from 1000 to 10000 with a step of 1000.

First, we fixed the number of individuals Ψ to 54 (i.e., 3 multiplies of Ω), and we varied the maximum number of iterations with improvement as follows: $\Gamma = 100$, 500, 1000, 1500, and 2000.

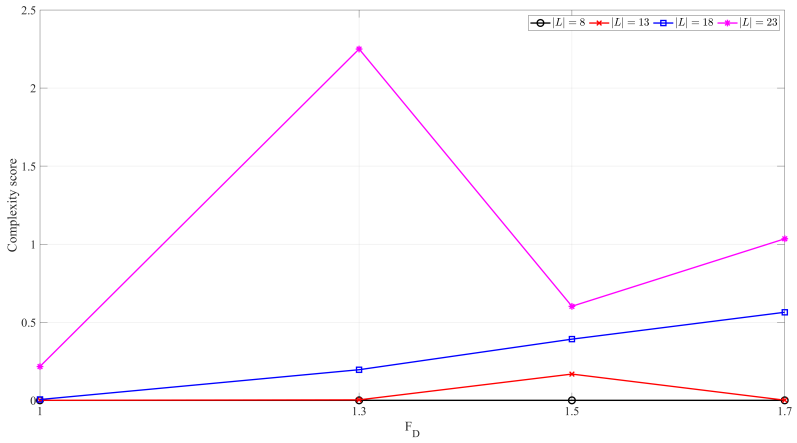

(a) Average complexity score as a function of the demand factor (F_D) for different numbers of ports

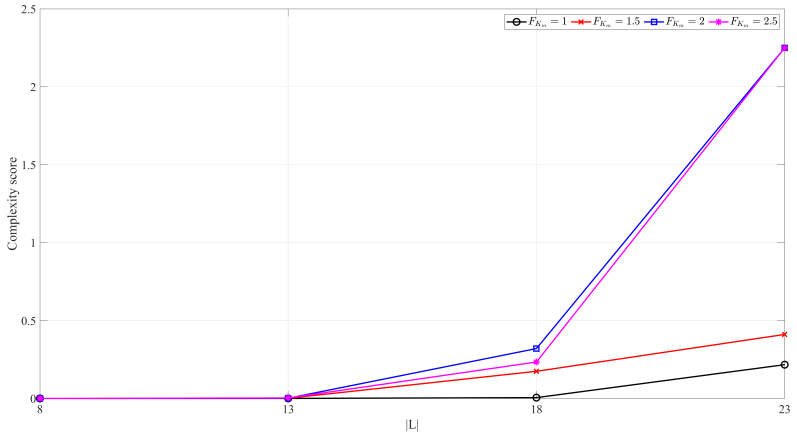

(b) Average complexity score as a function of the number of ports ($|L|$) for different vehicle factors F_{K_m}

Fig. 4: The average complexity score using the multimodal model.

Figure 5 shows the average impact of all instances (ten runs of each instance and the three objective functions; cost, emission and the biobjective formulation). Figure 5(a) shows the average relative difference in the objective value with respect to the best heuristic objective value found (i.e., the smallest among all iterations and Γ values) under different Γ values as a function of the number of iterations. Figure 5(b) shows the average computation time savings (with respect to the largest computation time) as a function of the number of iterations. In terms of quality, setting Γ to 500 provides, on average, the best solution quality at (and beyond) 5000 iterations. However, in terms

Table 3: Characteristics of the 21 instances

Instance	Size	$\|L\|$	F_D	$\|K_m\|$	Instance	Size	$\|L\|$	F_D	$\|K_m\|$
1	Small	8	1	11	12	Medium	23	1.5	46
2		8	1.3	13	13		28	1	40
3		8	1.5	14	14		28	1.3	50
4		13	1	17	15		28	1.5	60
5		13	1.3	21	16	Large	33	1	46
6		13	1.5	23	17		33	1.3	61
7	Medium	18	1	37	18		33	1.5	69
8		18	1.3	45	19		38	1	55
9		18	1.5	55	20		38	1.3	67
10		23	1	32	21		38	1.5	80
11		23	1.3	41					

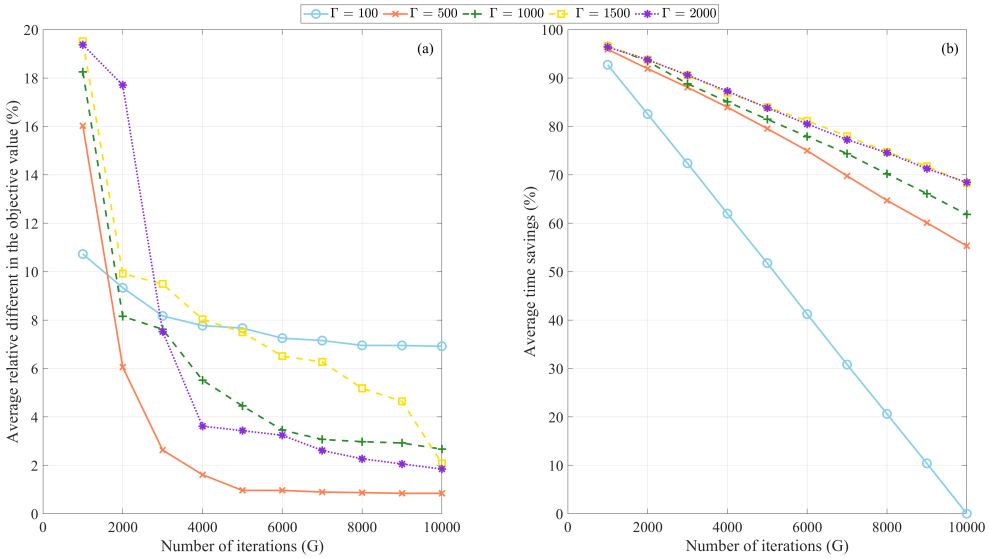

Fig. 5: Average relative difference in the objective value and time savings with respect to the best heuristic solution found as a function of the number of iterations for different numbers of iterations without improvement

of time savings, choosing $\Gamma = 2000$ or 1500 results in the fastest algorithm setting, with 83% at 5000 iterations compared to 96% at 1000 iterations. It is worth noting that setting $\Gamma = 500$ at 5000 iterations is 3.5% slower than that of $\Gamma = 2000$. Given that the difference is small and that the solution quality difference is more favorable, we chose to perform our experiments by using $\Gamma = 500$. Let us note that the higher the value of Γ is, the less there is a need for the algorithm to generate a new population, thus making it faster. However, this may lead to fewer opportunities to explore new potential individuals (through generating completely new populations) but a greater possibility of exploring modifications to the current individuals.

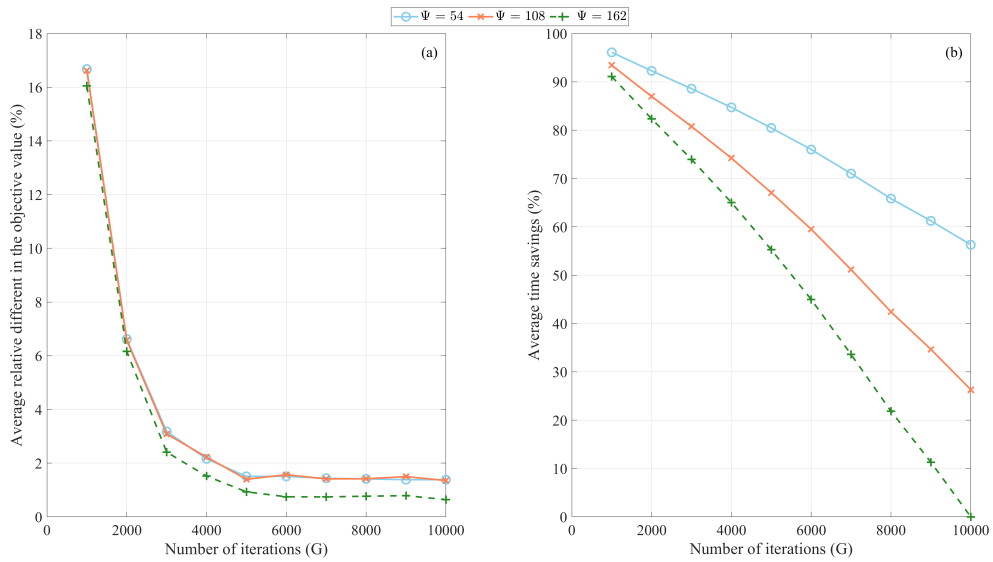

Fig. 6: Average relative difference in the objective value and time savings with respect to the best heuristic solution found as a function of the number of iterations for different numbers of individuals

Next, we explore the impact of the number of individuals in the population as follows: $\Psi = 54$, 108 and 162 (3, 6 and 9 multiplies of the number of operators Ω). In these experiments, we set Γ to 500, as it was found to perform well in terms of the solution quality. Figure 6 shows the average relative difference of the objective value with respect to the best solution found and the average time savings with respect to the slowest case. Figure 6(a) shows that the difference between the best solution found when using $\Psi = 54$ and when using $\Psi = 108$ is 0.02% at 5000 iterations, while the algorithm becomes slower as the time savings decrease from 80.46% to 67.06%. Using 162 individuals in the population decreases the time saved to 55.27% to improve the solution quality by approximately 0.06% on average (Figure 6(b)). Thus, in our analysis, we considered $\Psi = 54$ (3 multiplies of the number of operators Ω) as the population to achieve a balance between solution quality and computation time. Furthermore, in both experiments, we observe that on average, 5000 iterations are sufficient to reach an acceptable solution in a reasonable amount of time. Thus, we fix the number of iterations to 5000 in our further analysis.

6.3 Heuristic performance

We compare the heuristic results with those obtained by using the exact approach. The termination criterion for the exact approach is a 3-hour time limit. We ran the numerical experiments by using the 21 instances defined in Table 3 and the case study presented in Section 5 with its original demand as well as increased demands of 10,

20, 30, and 40%. All experiments were conducted by using $\Psi = 54$, $\Gamma = 500$ and $G = 5000$, as discussed in Section 6.2.

We used the computational time savings ($100 \times \frac{\text{Exact time - Heuristic time}}{\text{Exact time}}$) and the relative difference between the best exact and heuristic solutions ($100 \times \frac{\text{Heuristic best solution - Exact best solution}}{\text{Exact best solution}}$) as performance indicators. Since we repeated each experiment ten times, we considered averaging the relative differences (Avg RD) and time savings; consequently, we presented the relative difference standard deviations (RD std) to show the variability.

Tables 4, 5 and 6 show the performance of the multimodal model when using heuristics compared with that of the exact approach under cost minimization only, emission minimization only and the biobjective configuration. The relative difference (RD) under cost minimization (Table 4) ranged from 0.06% to 5.99%, with an average performance of 2.58% and low variability (average std = 0.47 and coefficient of variation of 0.18). The heuristic resulted in a relative difference between -0.08% and 3.25% under emission minimization (Table 5). The average relative difference is 1.37%, with a standard deviation of 0.35 and a coefficient of variation of 0.26. Notably, the exact approach failed to obtain a feasible solution for six instances under cost minimization and eight instances under emission minimization (Tables 4 and 5). The relative difference of the biobjective formulation in Table 6 is computed by multiplying the relative differences of the cost and emission by their importance weights. Let us note that in all instances, the objectives are assumed to have equal importance weights ($a_l = a_2 = 0.5$). The average relative difference is 0.27% (ranging from -2.14% to 2.70%), with an average standard deviation of 0.2 and a coefficient of variation of 0.73. This shows that the heuristic is capable of providing good quality solutions. It is also capable of finding feasible solutions for cases where the exact approach cannot be used. Table 7 shows the time savings of the multimodal model. The first three instances reached the optimal solution within five minutes when using the exact approach. Thus, the heuristic approach did not achieve any time savings (the heuristic run time ranged between 400 seconds and 600 seconds for these instances). The exact approach found the optimal solution for instances 4–6 and 10 under cost minimization within 1200 seconds. Thus, the heuristic managed to achieve time savings ranging from 15.20% to 45.87%. Table 7 shows that the heuristic approach provides an average time savings of 82.93%. In summary, the proposed population-based heuristic approach provides a high-quality solution within a short computational time.

7 Managerial insights

We highlight four managerial observations from the real-life study case presented in Section 5 to address the research questions.

Observation 1: Multimodal transportation relies heavily on inland waterway transportation, resulting in similar cost and emission values, yet the differences are significant.

We study the behavior of multimodal and single-mode models for high demand levels. We also compared the single-objective results with the multiobjective results.

Table 4: Exact and heuristic performance under the cost minimization formulation

Instance	Exact value	MIP gap (%)	Average heuristic value	Avg RD (%)	RD Std
1	7.05×10^4	0.00	7.14×10^4	1.16	0.04
2	2.38×10^4	0.00	2.38×10^4	0.14	0.01
3	2.73×10^4	0.00	2.79×10^4	2.12	0.06
4	3.33×10^4	0.00	3.33×10^4	0.06	0.01
5	4.14×10^4	0.00	4.14×10^4	0.10	0.06
6	4.52×10^4	0.00	4.55×10^4	0.62	0.01
7	7.45×10^4	0.89	7.68×10^4	3.20	0.87
8	9.22×10^4	0.40	9.67×10^4	4.97	0.97
9	1.03×10^5	1.32	1.08×10^5	4.42	0.67
10	6.25×10^4	0.00	6.51×10^4	4.12	1.23
11	8.84×10^4	1.44	9.24×10^4	4.54	1.06
12	1.01×10^5	2.29	1.04×10^5	3.29	0.74
13	8.68×10^4	4.47	8.85×10^4	1.95	0.24
14	*	*	1.19×10^5	*	*
15	*	*	1.25×10^5	*	*
16	1.11×10^5	10.99	1.12×10^5	0.82	0.46
17	*	*	1.30×10^5	*	*
18	1.47×10^5	9.54	1.52×10^5	3.13	0.87
19	*	*	1.25×10^5	*	*
20	*	*	1.53×10^5	*	*
21	*	*	1.69×10^5	*	*
Case study					
Base	6.49×10^4	1.40	6.62×10^4	2.03	0.48
+10% Demand	7.03×10^4	0.93	7.19×10^4	2.32	0.64
+20% Demand	7.63×10^4	0.82	7.84×10^4	2.77	0.41
+30% Demand	8.16×10^4	0.62	8.65×10^4	5.99	0.21
+40% Demand	8.64×10^4	1.05	8.98×10^4	3.85	0.28

* The exact approach could not find a feasible solution within the time limit.

In Figure 7, we increase the demand level from 100 to 140%. The figures in the first column compare inland waterway transportation with multimodal transportation under single-objective and biobjective configurations. The figures in the second column compare trucks with multimodal transportation under the same configurations. We observed that the results for the multimodal model and the single inland waterway transportation model were very close. This is because the model aims to transport by using inland waterways when demand is relatively high. That is, more inland waterway transportation is utilized to accommodate increased demand. However, in the same figure, we can see that the costs and emissions of trucks are higher than those of multimodal trucks. This is due to the mode restrictions in the truck-only case. We analyze the savings (in terms of cost or emissions) obtained by the multimodal model compared to the single mode (inland waterways or trucks). We compute the savings as the relative difference between the multimodal and single modes (e.g., the

Table 5: Exact and heuristic performance under the emission minimization formulation

Instance	Exact value	MIP gap (%)	Average heuristic value	Avg RD (%)	RD Std
1	1.46×10^6	0.00	1.47×10^6	0.85	0.06
2	5.82×10^5	0.00	5.92×10^5	1.65	0.02
3	6.61×10^5	0.00	6.63×10^5	0.41	0.01
4	7.02×10^5	1.15	7.09×10^5	0.91	0.02
5	9.94×10^5	3.15	1.00×10^6	0.78	0.47
6	1.12×10^6	2.78	1.15×10^6	2.77	0.84
7	1.69×10^6	2.12	1.72×10^6	1.64	0.71
8	1.92×10^6	1.94	1.98×10^6	2.96	1.02
9	2.91×10^6	2.32	2.94×10^6	1.16	0.08
10	1.72×10^6	1.10	1.77×10^6	3.05	0.98
11	2.05×10^6	1.09	2.12×10^6	3.25	0.86
12	2.65×10^6	0.87	2.67×10^6	0.55	0.18
13	2.19×10^6	2.56	2.21×10^6	0.98	0.67
14	*	*	2.16×10^6	*	*
15	*	*	1.98×10^6	*	*
16	*	*	1.78×10^6	*	*
17	*	*	2.24×10^6	*	*
18	*	*	2.17×10^6	*	*
19	*	*	2.30×10^6	*	*
20	*	*	2.19×10^6	*	*
21	*	*	2.26×10^6	*	*
Case study					
Base	1.29×10^6	0.02	1.31×10^6	1.61	0.21
+10% Demand	1.40×10^6	0.21	1.40×10^6	0.09	0.01
+20% Demand	1.49×10^6	0.18	1.49×10^6	-0.08	0.02
+30% Demand	1.54×10^6	0.07	1.55×10^6	0.77	0.01
+40% Demand	1.53×10^6	0.06	1.55×10^6	1.24	0.21

* The exact approach could not find a feasible solution within the time limit.

cost savings when moving from inland waterways to multimodal waterways is calculated as $100 \times \frac{(c_{\text{inland}} - c_{\text{multimodal}})}{c_{\text{inland}}}$). Using the multimodal model results in cost savings between 0.40% and 1.08%, which are statistically significant (right-tailed t test: mean savings are greater than 0, p value = 0.0024), and emission savings between 1.02% and 2.38%, which are statistically significant (same test, p value = 0.0008). However, in the biobjective configuration, the multimodal model results are -0.37% and 0.39% (not statistically significant, p value = 0.64), and the emission savings are between 0.11% and 1.67% (statistically significant, p value = 0.01). Replacing trucks only with a multimodal transportation system results in an average cost savings of 51.64% and an average emission savings of 88.99% in both the single and biobjective cases, which is statistically significant, with a p value = 0. Let us note that all differences were normally distributed according to the Shapiro–Wilk test, with a p value > 0.2 for all the patients. In general, this shows that while differences between inland waterway

Table 6: Exact and heuristic performance under the biobjective formulation

Instance	Exact		MIP gap (%)	Heuristic		Avg RD (%)	RD Std
	Cost	Emission		Avg cost	Avg emission		
1	7.20×10^4	1.48×10^6	0.00	7.26×10^4	1.47×10^6	0.21	0.02
2	2.43×10^4	5.87×10^5	0.00	2.44×10^4	5.86×10^5	0.16	0.02
3	2.77×10^4	6.67×10^5	0.00	2.78×10^4	6.81×10^5	1.21	0.01
4	3.36×10^4	7.16×10^5	1.65	3.37×10^4	7.18×10^5	0.38	0.12
5	4.18×10^4	1.00×10^6	4.21	4.22×10^4	1.05×10^6	2.70	0.26
6	4.57×10^4	1.12×10^6	4.56	4.58×10^4	1.14×10^6	0.97	0.03
7	7.82×10^4	1.80×10^6	1.45	7.88×10^4	1.82×10^6	1.07	0.30
8	9.86×10^4	1.95×10^6	2.65	9.92×10^4	1.97×10^6	0.89	0.08
9	1.37×10^5	3.27×10^6	7.62	1.38×10^5	3.33×10^6	1.21	0.42
10	7.00×10^4	1.80×10^6	2.35	7.02×10^4	1.83×10^6	0.74	0.36
11	1.10×10^5	2.09×10^6	4.14	1.10×10^5	2.08×10^6	-0.49	0.27
12	1.25×10^5	2.89×10^6	19.25	1.25×10^5	2.85×10^6	-0.86	0.38
13	1.17×10^5	2.40×10^6	21.36	1.17×10^5	2.31×10^6	-2.14	0.43
14	*	*	*	1.33×10^5	2.34×10^6	*	*
15	*	*	*	1.43×10^5	2.10×10^6	*	*
16	*	*	*	1.19×10^5	1.93×10^6	*	*
17	*	*	*	1.45×10^5	2.30×10^6	*	*
18	*	*	*	1.68×10^5	2.25×10^6	*	*
19	*	*	*	1.42×10^5	2.41×10^6	*	*
20	*	*	*	1.58×10^5	2.23×10^6	*	*
21	*	*	*	1.73×10^5	2.32×10^6	*	*
Case study							
Base	6.65×10^4	1.29×10^6	3.12	6.66×10^4	1.31×10^6	0.97	0.17
+10% Demand	7.11×10^4	1.43×10^6	2.15	6.92×10^4	1.41×10^6	-2.04	0.08
+20% Demand	7.76×10^4	1.49×10^6	1.87	7.76×10^4	1.47×10^6	-0.69	0.30
+30% Demand	8.24×10^4	1.55×10^6	1.41	8.28×10^4	1.57×10^6	0.75	0.18
+40% Demand	8.81×10^4	1.53×10^6	2.11	8.82×10^4	1.52×10^6	-0.09	0.16

* The exact approach could not find a feasible solution within the time limit.

transportation and multimodal transportation are very small, they are still significant in most objective settings. Additionally, the multimodal transportation system relies heavily on inland waterway transportation as demand increases due to capacity requirements, which explains the close difference between the two.

Observation 2: Although the increase in the lock time increases the total cost, the multimodal model reduces this impact by 23% compared to the inland waterway transportation model.

We analyzed the effect of longer lock times due to traffic jams on the canal system. We varied the lock times from 40 to 120 minutes in 20-minute steps. An increase in the number of lock times requires more inland waterway transportation when demand is too high; in practice, this approach increases the likelihood of long queues at the lock, further increasing the number of lockage times. We also illustrate how the multimodal

Table 7: Time savings of using the heuristic method

Instance	Cost minimization Avg	std	Emission minimization Avg	std	Bi-objective minimization Avg	std
1	*	*	*	*	*	*
2	*	*	*	*	*	*
3	*	*	*	*	*	*
4	20.65	0.02	89.05	0.61	88.82	0.26
5	19.74	0.16	95.92	0.24	94.81	0.40
6	45.87	0.21	91.29	0.49	88.31	0.78
7	87.03	0.01	91.83	0.07	91.15	0.29
8	84.37	0.02	94.50	0.43	84.29	0.61
9	85.52	0.07	87.42	0.23	94.13	0.83
10	15.20	0.21	88.59	0.29	85.41	0.44
11	88.03	0.01	84.48	0.51	93.15	0.94
12	85.14	0.03	93.63	0.30	93.89	0.56
13	96.01	0.05	94.98	0.10	88.97	0.62
14	94.00	0.08	92.63	0.16	88.82	0.73
15	93.18	0.08	91.23	0.23	95.89	0.80
16	96.86	0.06	91.52	0.36	84.57	0.89
17	90.04	0.06	92.39	0.56	90.78	0.61
18	89.07	0.03	85.03	0.19	86.18	0.60
19	95.91	0.03	87.83	0.13	87.83	0.97
20	91.86	0.05	87.59	0.24	90.38	0.54
21	94.15	0.07	94.68	0.28	89.64	0.04
Case study						
Base	75.96	0.28	78.65	0.63	74.95	0.05
+10% Demand	74.53	0.18	79.45	0.18	75.67	0.29
+20% Demand	70.52	0.09	72.65	0.15	71.65	0.03
+30% Demand	72.20	0.65	73.26	0.11	71.28	0.32
+40% Demand	68.58	0.37	70.41	0.54	68.51	0.09

* No time savings as the exact solution was obtained within five minutes.

model minimizes costs. The results are shown in Figure 8. Different scenarios for longer lock times do not influence the single-truck model because they influence only the optimal solutions for models involving inland waterway transportation. Emissions are also not affected. However, costs are affected. By comparing the results while minimizing costs, we can see that the costs of inland waterway transportation increase faster than those of multimodal transportation systems (Figure 8).

The total costs for inland waterway transportation increase by €165.7 per minute of increase in the lock time (linear fit, with a coefficient of determination of 0.999) compared with €126.2 per minute when using multimodal transportation (linear, with a coefficient of determination of 0.992). This is an approximately 23.8% reduction in the cost per minute of lock time. The multimodal model absorbs the impact of the increase in lock time due to the greater flexibility in routing decisions provided by the availability of trucks as an option. The findings demonstrate the cost-saving potential of the different modes. Figure 8(b) shows the relative difference in the cost

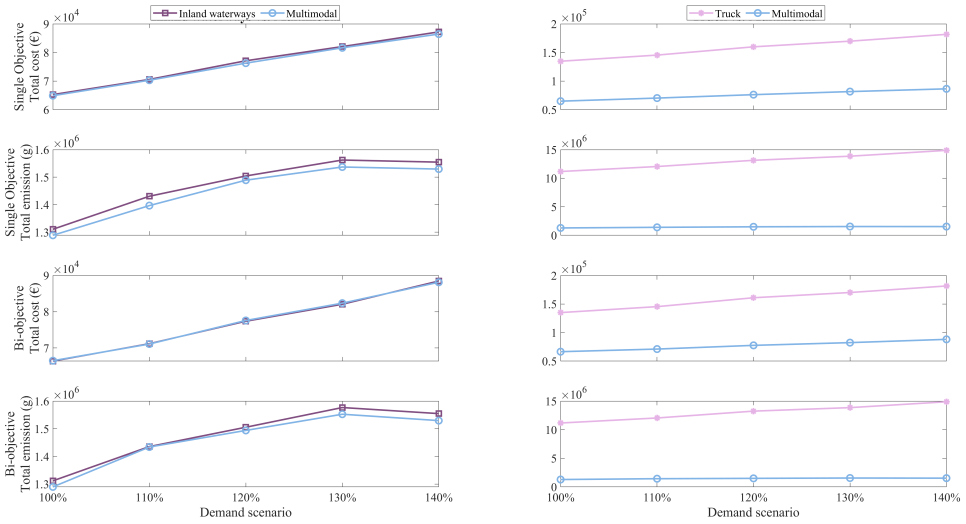

Fig. 7: Objective function values for inland waterways, trucks and multimodal transportation under various demand levels

with respect to the baseline case of 40 minutes of lock time. The figure shows that the cost increases, on average, by 5.05% for inland waterways and by 3.71% for multimodal transportation for each 20-minute increase in lock time. We conclude that multimodal transportation provides a statistically significant decrease in cost compared to inland waterway transportation (normal with p value = 0.67, one-tailed paired t test with p value = 0.03).

Observation 3: Infrastructure failures impose higher costs of nearly 28% per day; in this case, multimodal transportation is more efficient than a single transportation mode.

We investigated the effect of the failure of each lock in the system on performance. This analysis allows decision-makers to know the effects of their respective port locations if one lock fails. Only some scenarios allow inland waterway transportation to fulfill the total demand (see Table E3 in the Appendix). Others must be served by inland waterway transportation and trucks.

Figure 9 shows the total cost of inland waterway transportation and multimodal transportation under the various lock failure scenarios. Let us note that scenario 0 represents the baseline case with no lock failures. Lock failure under scenarios 4 and 7–12 results in infeasible service due to accessibility issues (see Table E3). The total cost under multimodal transportation is significantly lower than that under inland waterway transportation (normal with p value = 0.2, one-tailed paired t test with p value = 0.045). As Figure 9 shows, minimizing the total costs leads to a maximum increase of 27.59% of the costs when using inland waterway transportation (see the increase in the total cost of scenario 1). This increase is with respect to the baseline

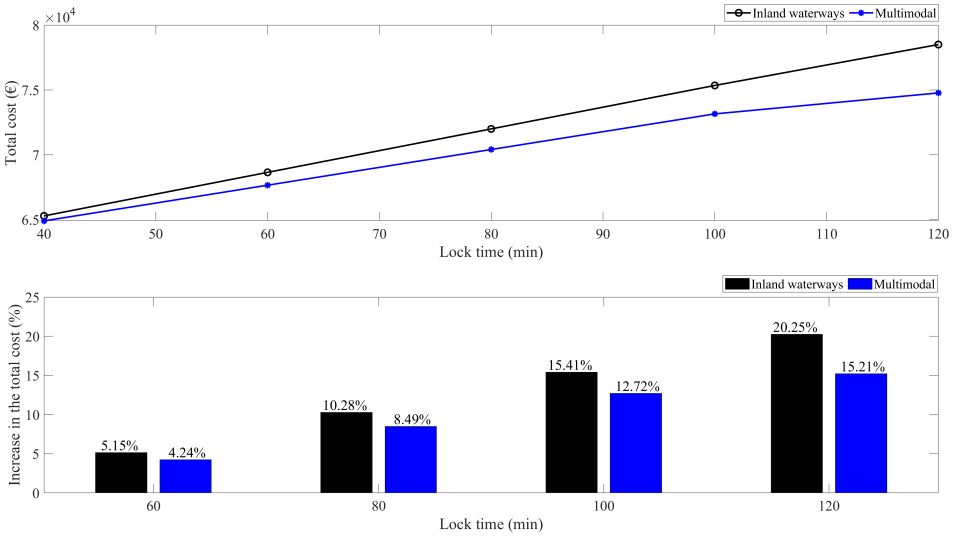

Fig. 8: Effect of varying lock times on total costs

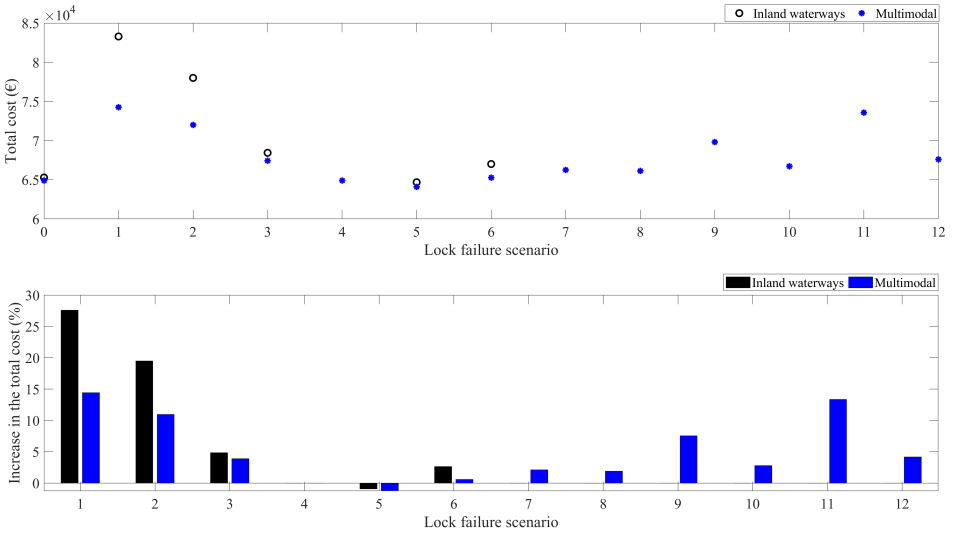

Fig. 9: Effects of lock failure scenarios on total costs while minimizing only costs

scenario (scenario 0 - no lock failure). The locks in scenarios 1, 2, and 3 are the most critical due to the high increase in the cost and require a higher priority to modernize the infrastructure or maintenance operations.

Scenario 5 was of interest. We see that taking the alternative northern route via Rhein-Lippe is more beneficial even if the locks fail. The reason for this is the high

demand for Marl and the number of locks that have to be passed to reach Marl. To achieve cost efficiency, decision-makers should select a route via Rhein-Lippe for accessing the port, considering the high demand for chemical products in this region. The multimodal model allows savings of up to 78% compared with a single model. Infrastructure dependency demonstrates the benefits of having an additional mode. Figure 9 shows that inland waterway transportation results in a 10.72% increase in the total cost on average in Scenarios 1, 2, 3, 5 and 6 compared to an average increase of 5.72% when using multimodal transportation.

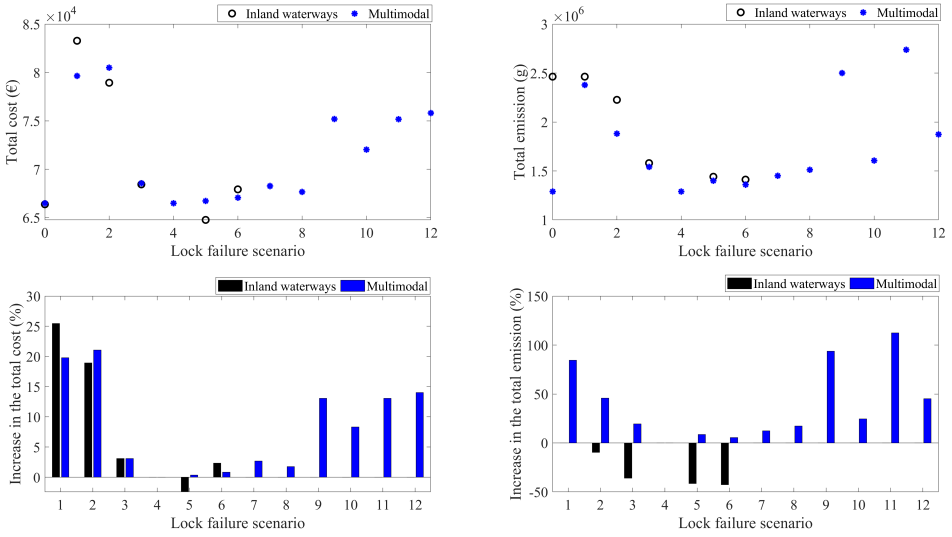

Fig. 10: Effects of lock failures for the biobjective model

Figure 10 shows the effect of minimizing both costs and emissions (the biobjective formulation). We can again observe the greatest difference for scenarios 1 to 3. The total cost and emissions when using the multimodal model are lower than those of inland waterway transportation. The mean total cost difference is not significantly different between the two models (normal with p value = 0.54, two-tailed paired t test with p value = 0.87). The mean total emission was found to be significantly lower in the multimodal model (not normal with p value = 0.006, one-tailed sign test with p value = 0.03). The trade-off between emissions and costs is clear. For some scenarios, higher costs are compensated for by the use of fewer emissions. These results show the variations in both objectives, which are further discussed in the next section. The increase in emissions under the multimodal model in Figure 10 is with respect to the baseline scenario (no lock failure). However, the increase in emissions under these scenarios is still lower than that under inland waterway transportation. Decision-makers should assign different weights to both objectives depending on the importance and prioritization of the decision.

Observation 4: Multimodal transportation provides a faster emission reduction rate when the total cost increases by 1%.

Here, we calculated the cost of reducing emissions using inland waterway ships, trucks, and multimodal transportation. The analysis is performed by varying a_1 and a_2 in Equation (44), which results in different Pareto optimal solutions. We emphasize that the chosen scalarization method was selected due to the availability of decision-maker preferences, its simplicity, and its suitability for the heuristic approach. Although this method might not yield every Pareto optimal point, it aligns well with our analysis, given that the decision-maker's preferences are predefined. Moreover, since the decision-maker predetermines the importance of each objective function, this approach adequately provides the necessary insights for informed decision-making. The relative difference between any point on the Pareto optimal set and its subsequent point (next point found on the front) is then calculated as $(\frac{c_i - c_{i+1}}{c_i}, \frac{e_i - e_{i+1}}{e_i})$, where i is the current point, $i+1$ is the next (subsequent) point on the front, and c_i and e_i are the cost and emission values of point i, respectively. All the resulting relative differences are averaged. Figure 11 shows the total cost and the total emission when varying the importance weights from 0 to 1 with an increment of 0.1 when using the three models (inland waterways, trucks and multimodal). All solutions were checked, and only non-dominated unique solutions were retained. Figure 11 illustrates the trade-off between the total cost and total emissions for each model. A 1% reduction in emissions increased the total cost by 1.32%, 2.93%, and 0.90%, respectively, when using inland waterway transportation, trucks, and multimodal transportation. This highlights that using multimodal transportation helps reduce emissions while incurring lower costs when compared to other options. The findings also highlight that if decision-makers give less preference to the environment, a reduction in cost is associated with a greater rate of increase in emissions (compared with the ideal case of minimizing emissions) when using multimodal transportation. That is, reducing costs by 1% results in increases in emissions of 0.76%, 0.34%, and 1.12% for inland waterway ships, trucks, and multiple modes, respectively. It is also true that increasing costs by 1% reduces emissions by 1.12% when using multimodal transportation. These percentages reflect the rate of change or how quickly costs or emissions increase and decrease.

We utilized the Wilcoxon rank sum test (the data were not normally distributed, p value <0.05) to compare the Pareto points of each transportation mode and to assess whether these differences were statistically significant. We found that the differences in cost and emissions between inland waterways and multimodal transportation are not statistically significant (p value>0.08). This means that although multimodal waterways provide slightly better trade-offs than do inland waterways, these differences are not statistically significant and that both modes have comparable efficiencies in terms of balancing cost and emissions. In contrast, the differences between multimodal transportation and trucks are statistically significant, indicating that multimodal transportation or inland waterway transportation offers a more cost-effective solution for reducing emissions than trucks.

To assess the heuristic performance in generating the biobjective solutions, we used the hypervolume indicator to quantify the volume of the objective function space covered by the Pareto points with respect to a reference point. This measure indicates

Table 8: Hypervolume results of the exact and heuristic Pareto optimal sets

Transportation mode	Hypervolume		RD (%)
	Exact	Heuristic	
Inland waterways	767895800	763730000	0.54
Truck	25730000	25730000	0.00
Multimodal	10322413400	10256591500	0.64

how close the heuristic Pareto set is to the exact approach Pareto set. We used the "ecr" package in R Studio to calculate the nondominated hypervolume of the Pareto optimal set by using the exact and heuristic approaches (Table 8). The relative difference in the hypervolume between the two sets was very small (less than 1%), meaning that the two sets had very similar results.

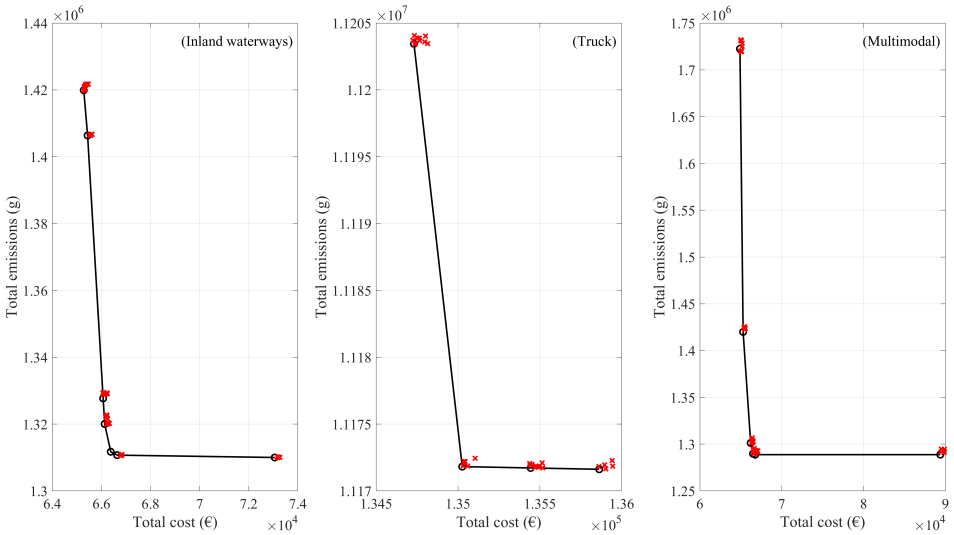

Fig. 11: Total cost versus total emissions for each transportation mode. The circles 'o' and 'x' represent the solutions obtained by using the exact and heuristic approaches, respectively.

8 Conclusion

In this study, we gained insights into how multimodal transportation can be used in the West German region, more precisely, what impact the choice of transportation mode has on total costs and emissions. Furthermore, the viability of this choice was evaluated under different waterway infrastructure failure scenarios, which affected

the multimodal balance. While using a cost function proposed by the German Federal Institution and an emission function based on ISO14083, the results are reliable regarding historic routing problems in the company and cost estimations of transportation by the German Federal Institution. To create different scenarios, we utilized actual data from the West German canal system and its 16 ports and 14 locks. Managerial insights, such as the effect of infrastructure failures on the logistics flow in the region, allow decision-makers to know the monetary and emission-related costs for their companies. Moreover, the effect of varying demand on the network was analyzed, and decision-makers were able to understand how increased demand volumes impact the cost and emissions of different transportation modes. We also identified additional costs incurred when the number of lock times increased and demonstrated the advantages of using the two modes. We also describe the effects of using only one objective optimization compared to that of the biobjective function and its effect on the objective values. The proposed heuristic approach for our model leads to an average time savings of 82% and acceptable accuracy with a relative difference of less than 5% when compared to that of the best exact solution found. This formulation allowed us to generate good results within an acceptable time.

This study was based on the literature on transportation and sustainable routing problems. To the best of our knowledge, there is no algorithm that selects transshipment nodes in the models, as we do here. The biobjective approach allows decision-makers to consider the future pricing of emissions. Single biobjective and multimodal biobjective transportation models can be applied to any waterway system with multimodal hubs subject to computational boundaries, such as the inland waterway system of the Netherlands. Business decision-makers benefit from obtaining transparency about the expected cost increase in their supply relations regarding the current state of infrastructure availability. Public decision-makers benefit from the possibility of prioritizing the operation of infrastructure regarding the monetary and the emission costs of infrastructure failures in the system. The model determines the quantitative evaluation of modal shift and of rerouting in response to infrastructure failure as a risk mitigation strategy that can be integrated into a broader risk management or supply chain resilience perspective by decision-makers. The analysis in this study allows a better understanding of the impact of varying demands on transportation mode choice, and the effects of varying lock times and infrastructure failure can be interpreted by decision-makers with this model. The proposed formulation allows the decision-maker to optimize the transshipment port, delivery routes, and quantities, as well as the number of vehicles used in each mode, based on a reasonable setting of parameters. Moreover, other data on stake-holding industries in the West German region, such as the coal, arc, and stone industries, can be used to obtain insights into the optimal transportation mode choice. This analysis allows decision-makers to gauge the locks and bridges that can have the most substantial impact on costs and emissions in the event of failure. System cost levels are minimized under the assumption that shippers cooperate and consolidate their shipments for optimal cost-efficient utilization. This behavior, namely, tramp shipping, is evident in short-sea shipping and inland waterway transport. However, the real costs of the transport system and the adverse effects of infrastructure failure are greater in practice, as the system contains

more underutilized point-to-point transport. The algorithm is a single-product, multivehicle model. In the future, considering multiple products of similar industries can be advantageous for decision-makers. However, considering a bundle of 10 trucks can be criticized because it leads to higher costs if the capacity is not fully used. The formulation complexity is significantly affected by the problem size because the runtime exponentially increases with the addition of new ports and vehicles. As transshipment emissions (e.g., those stemming from prolonged storage times) are difficult to account for, this aspect was not considered in the case study. This aspect can be explored in future studies. An advantage of the model is that it allows the addition of new transportation modes without changing constraints; therefore, adding rail can benefit decision-makers because it is a sustainable substitution, especially for trucks. Furthermore, speed optimization can be added to reduce emissions and costs. It is of interest to implement the algorithm in other case studies, such as the coal, ore, and stone industries. Moreover, it is of interest to evaluate the algorithm with another entrance port, that is, the depot, in the model to analyze its influence on the network. We also performed a sensitivity analysis of the vehicles and their effect on the optimal solution and runtime. Another scenario may be the development of new technologies in the truck market with greener propulsion technologies. Let us note that decision-makers can use the results of this study for the allocation of production sites at a strategic level because of the vulnerability of the existing infrastructure.

Declarations

- Funding: The project (FKZ: 13N14700) is partially funded by the German Federal Ministry of Education and Research (BMBF).
- Conflict of interest/Competing interests: not applicable
- Availability of data and materials: Available upon request
- Code availability: Available upon request

Appendix A Problem complexity

The problem complexity is characterized in Lemma 1:

Lemma 1. *The multimodal transportation problem with transshipment port allocation defined in Equations (18) – (41) is an NP-hard problem.*

Proof. We prove that this problem is an *NP*-hard by reducing it to a well-known *NP*-hard problem (Arora & Barak, 2009). Let $m = 1$ and $\sum_{m \in M} K_m = 1$, that is, one vehicle with unlimited capacity is available in the service. Thus, Constraints (26) and (31) can be eliminated. Having one vehicle requires that one service be possible and that a secondary service (transshipment) is impossible, resulting in the removal of decision variables $T_i^{k,m}$ and $UQ_i^{k,m}$ and their associated constraints. Since all demand must be satisfied (Constraint (30)), Constraint (21) becomes redundant as all ports are forced to be visited by the same vehicle. Thus, decision variables $y_i^{k,m}$, $Q_i^{k,m}$ and $f_{i,j}^{k,m}$

become unnecessary, and their associated constraints can be removed. This reduces this problem to the well-known traveling salesman problem, which is *NP*-hard; see (Garey & Johnson, 1979; Jungnickel, 1999), among others. Since the simplified case is *NP*-hard, the general case presented in this work is also *NP*-hard, which completes the proof. □

Appendix B Reducing multimodal transportation to a single-mode model

The multimodal model can be reduced to a single model for inland waterway transportation or trucks. In the single model, we no longer have a virtual depot but rather an actual ordinary depot of the network. Input data, such as the distances for inland waterway transportation, trucks, and demand, must be adapted. The decision variables $UQ_i^{k,m}$ and $T_i^{k,m}$ were not needed. Moreover, some constraints remain unchanged, others need to be adapted, and others are not needed. The following equations are subject to the same objective function and are unchanged: (20), (21), (22), (25), (26), (29) and (30). The constraints (23), (27), (28), and (31) are changed to (B1), (B2), (B3), and (B4), respectively.

$$S \times y_i^{k,m} \leq Q_i^{k,m} \leq D_i \times y_i^{k,m} \quad \forall i \in L \setminus \{i_0\}, \quad \forall k \in K_m \quad \forall m \in M, \tag{B1}$$

$$\sum_{j \in L} f_{i,j}^k = \sum_{j \in L} f_{j,i}^{k,m} - Q_i^{k,m}, \quad \forall i \in L, \quad \forall k \in K_m, \quad \forall m \in M, \tag{B2}$$

$$\sum_{j \in L} f_{i_0,j}^k = \sum_{j \in L} Q_j^{k,m}, \quad \forall k \in K_m, \quad \forall m \in M, \tag{B3}$$

$$\sum_{i \in L} Q_i^{k,m} \leq C^{k,m} \quad \forall k \in K_m \quad \forall m \in M. \tag{B4}$$

Constraint (B1) ensures that if we do not select the port, then the quantity equals zero. If we select the port to be visited, then the quantity is nonzero, less than or equal to the demand. Constraint (B2) defines the flow from i to j as the flow that enters i from all possible j values minus the quantities. Constraint (B3) defines the first flow, which is the total loaded quantity, and Constraint (B4) ensures that the total quantities loaded in each vehicle do not exceed its capacity.

Appendix C Heuristic subroutines

In this section, we detail the various subroutines used in the proposed heuristic. The connections between different subroutines are illustrated in Figure C1.

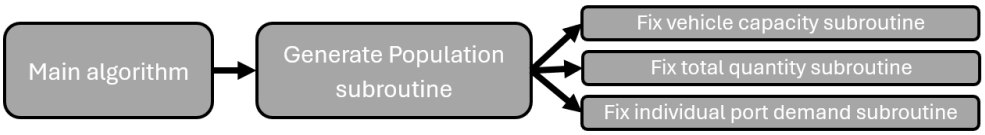

Fig. C1: Main algorithm and subroutines connections.

C.1 Population generation Subroutine

The **Population Generation** subroutine (shown in Algorithm 3) generates randomly feasible initial individuals. The population generation subroutine creates two chromosomes for each individual (ψ), called the "route chromosome" and the "quantity chromosome." The route chromosome carries information about the vehicle type and the sequence of the port visit route, and the quantity chromosome carries information about the quantity delivered to each port and the transshipment quantities to be transported by using another transportation model. First, vehicle information is generated by randomly deciding the number of vehicles (NV_ψ) and the type of each vehicle ($m \in M$). The route is then generated by randomly choosing the number and sequence of ports visited (NP_ψ^{veh} and $\text{Route}_\psi^{\text{veh}}$) by each vehicle. The visited ports are created randomly such that a vehicle cannot visit the same port more than once, satisfying Constraint (20). Likewise, the sequence in the route chromosome implies the satisfaction of Constraint (20). Finally, each vehicle is loaded with a random quantity for each visited port, and the information is stored on the quantity chromosome. Once the vehicle information, route sequence, and quantity delivered are generated for each individual, the algorithm compares the total loaded quantity of each vehicle with its capacity. If a violation is detected, it is called the **Fix Vehicle Capacity** subroutine, which reduces the total loaded quantity and ensures the fulfillment of the model constraint (31). Subsequently, the total quantity carried by all vehicles is compared with the total demand (Constraint (30)). If a violation is detected, then the **Fix Total Quantity** subroutine is called. Finally, it initializes the transshipment quantity (stored in the quantity chromosome) and checks whether the total quantity delivered to each port fulfills the demand of the port. The **Fix Individual Quantity** subroutine is used to fix any violations in Constraint (30).

C.2 Fix vehicle capacity subroutine

The **Fix Vehicle Capacity** subroutine (Algorithm 4) is called during feasible population initialization when a vehicle within an individual (potential solution) has a quantity greater than its capacity. The subroutine calculates the excess quantity carried (Q^+) as the difference between the total quantity loaded and the vehicle capacity.

Algorithm 3 Population generation subroutine

Input: Context-related, vehicle-related, heuristic-related parameters, Ψ
Output: $\mathcal{P}$: an initial feasible population of Ψ individuals ▷ Generate initial individuals
for $\psi \leftarrow 1$ **to** Ψ **do**
    decide randomly the number of vehicles to be used (NV_ψ); $NV_\psi \leq \sum_{m \in M} |K_m|$
    for $veh \leftarrow 1$ **to** NV_ψ **do**
        decide randomly the vehicle type ($m \in M$)
        decide randomly the number of ports (NP_ψ^{veh}) to be included in the vehicle route ($Route_\psi^{veh}$)
        select randomly NP_ψ^{veh} ports and **add** them to $Route_\psi^{veh}$
        for $j \leftarrow 1$ **to** NP_ψ^{veh} **do**
            load vehicle veh with a random quanitity ($Q^{veh}_{\psi,Route^{veh}_{\psi,j}}$) for port $Route^{veh}_{\psi,j}$, calculated as
            $Q^{veh}_{\psi,Route^{veh}_{\psi,j}} = \mathbf{rand}() \times D_{Route^{veh}_{\psi,j}}$ ▷ where **rand**() represents a randomly generated number between 0 and 1.
        end for
        calculate the total qunatity ($\sum_{j=1}^{NP_\psi^{veh}} Q^{veh}_{\psi,Route^{veh}_{\psi,j}}$) carried by vehicle veh and **compare** it with the vehicle capacity (C^{veh})
        if $\sum_{j=1}^{NP_\psi^{veh}} Q^{veh}_{\psi,Route^{veh}_{\psi,j}} > C^{veh}$ **then**
            Fix Vehicle Capacity subroutine
        end if
    end for
    calculate the total quantity $\left(\sum_{veh=1}^{NV_\psi} \sum_{j=1}^{NP_\psi^{veh}} Q^{veh}_{\psi,Route^{veh}_{\psi,j}}\right)$ and **compare** it with the total demand ($\sum_{j=1}^{|L|} D_j$)
    if $\sum_{veh=1}^{NV_\psi} \sum_{j=1}^{NP_\psi^{veh}} Q^{veh}_{\psi,Route^{veh}_{\psi,j}} \neq \sum_{j=1}^{|L|} D_j$ **then**
        Fix Total Quantity subroutine
    end if
    initialize unloaded quantities UQ_ψ^{veh}
    for $j \leftarrow 1$ **to** NP_ψ^{veh} **do**
        if $\sum_{veh=1}^{NV_\psi} Q^{veh}_{\psi,Route^{veh}_{\psi,j}} - \sum_{veh=1}^{NV_\psi} UQ^{veh}_{\psi,Route^{veh}_{\psi,j}} - D_{Route^{veh}_{\psi,j}} \neq 0$ **then**
            Fix Individual Quantity subroutine
        end if
    end for
end for

The algorithm then randomly selects a port from the visited port list of the vehicle ($\text{Route}^{\text{veh}}_{\psi,\text{rnd}}$) such that the quantity transported to that port is nonzero. The selected port quantity ($Q^{\text{veh}}_{\psi,\text{Route}^{\text{veh}}_{\psi,\text{rnd}}}$) is reduced by Q^{+}. If Q^{+} is larger than $Q^{\text{veh}}_{\psi,\text{Route}^{\text{veh}}_{\psi,\text{rnd}}}$, $Q^{\text{veh}}_{\psi,\text{Route}^{\text{veh}}_{\psi,\text{rnd}}}$ is set equal to zero to avoid a negative quantity. The algorithm terminates when the vehicle capacity constraint is not violated.

Algorithm 4 Fix vehicle capacity subroutine

Input: NP^{veh}_{ψ}, $Q^{veh}_{\psi,Route^{veh}_{\psi,j}}$, C^{veh}
Output: $Q^{veh}_{\psi,Route^{veh}_{\psi,j}}$
while $\sum_{j=1}^{NP^{veh}_{\psi}} Q^{veh}_{\psi,Route^{veh}_{\psi,j}} > C^{veh}$ **do** ▷ calculate excess Q
    $Q^{+} \leftarrow \sum_{j=1}^{NP^{veh}_{\psi}} Q^{veh}_{\psi,Route^{veh}_{\psi,j}} - C^{veh}$
    select randomly (rnd = **randi**($[1\ NP^{veh}_{\psi}]$)) a port ($Route^{veh}_{\psi,rnd}$) such that $Q^{veh}_{\psi,Route^{veh}_{\psi,rnd}} > 0$ ▷ where **randi**($[1\ NP^{veh}_{\psi}]$) returns a random integer between 1 and NP^{veh}_{ψ} that represents a port within the route
    $Q^{veh}_{\psi,Route^{veh}_{\psi,rnd}} \leftarrow \max\{0, Q^{veh}_{\psi,Route^{veh}_{\psi,rnd}} - Q^{+}\}$
end while
return $Q^{veh}_{\psi,Route^{veh}_{\psi,j}}$.

C.3 Fix total quantity subroutine

After the **Population Generation** subroutine fixes the vehicle capacity issues by calling the **Fix Vehicle Capacity** subroutine, the total demand is compared with the total loaded quantity for all vehicles. Once a violation is detected, the **Fix Total Quantity** subroutine (Algorithm 5) is called. This algorithm is based on two cases. The first case is the case of an excess quantity (Q^{+}) that exceeds the total demand. The algorithm selects the vehicle with the lowest load and then selects a visited port on the route of the selected vehicle. Subsequently, it reduces the loaded quantity to that port to either zero or by Q^{+}. The selection of the vehicle with the lowest load helps reduce the number of vehicles used. Let us note that if a vehicle carries no quantity, it is excluded from the search. The second case represents the situation in which the total quantity loaded is less than the total demand (called the shortage case), in which case the missing quantity (Q^{-}) is calculated as the difference between the total demand and the total quantity loaded on the vehicle. The remaining capacity of each vehicle was calculated, and vehicles with no remaining capacity were excluded. This decision led to two possible scenarios. In the first scenario, where all used vehicles have no remaining capacity, a new vehicle is added of a randomly available type, and random ports are assigned. The total load of this new vehicle can be calculated as the maximum between the vehicle's capacity and Q^{-}, which is then distributed randomly among the assigned ports. In the second scenario, where some vehicles are not fully

utilized, select the vehicle with the lowest utilization and transfer to a random port a minimum quantity between the vehicle's remaining capacity and Q^-. The algorithm terminates when the total demand is satisfied and returns the updated individual chromosomes to the **Population Generation** subroutine.

Algorithm 5 Fix total quantity subroutine

Input: $Route_{\psi},\ Q_{\psi},\ NP_{\psi},\ NV_{\psi},\ C,\ D,\ L$
Output: $Route_{\psi},\ Q_{\psi},\ NP_{\psi},\ NV_{\psi}$
while $\sum_{veh=1}^{NV_{\psi}} \sum_{j=1}^{NP_{\psi}^{veh}} Q_{\psi,Route_{\psi,j}^{veh}}^{veh} \neq \sum_{j=1}^{|L|} D_j$ **do**
    while $\sum_{veh=1}^{NV_{\psi}} \sum_{j=1}^{NP_{\psi}^{veh}} Q_{\psi,Route_{\psi,j}^{veh}}^{veh} > \sum_{j=1}^{|L|} D_j$ **do**
        $Q^{+} \leftarrow \sum_{veh=1}^{NV_{\psi}} \sum_{j=1}^{NP_{\psi}^{veh}} Q_{\psi,Route_{\psi,j}^{veh}}^{veh} - \sum_{j=1}^{|L|} D_j$
        Exclude a vehicle veh if $\sum_{j=1}^{NP_{\psi}^{veh}} Q_{\psi,Route_{\psi,j}^{veh}}^{veh} = 0$
        Select vehicle veh with lowest $\sum_{j=1}^{NP_{\psi}^{veh}} Q_{\psi,Route_{\psi,j}^{veh}}^{veh}$
        Select randomly ($rnd =$ **randi**($[1\ NP_{\psi}^{veh}]$)) a port ($Route_{\psi,rnd}^{veh}$) such that $Q_{\psi,Route_{\psi,rnd}^{veh}}^{veh} > 0$
        $Q_{\psi,Route_{\psi,rnd}^{veh}}^{veh} \leftarrow \max\{0, Q_{\psi,Route_{\psi,rnd}^{veh}}^{veh}\} - Q^{+}$
    end while
    while $\sum_{veh=1}^{NV_{\psi}} \sum_{j=1}^{NP_{\psi}^{veh}} Q_{\psi,Route_{\psi,j}^{veh}}^{veh} < \sum_{j=1}^{|L|} D_j$ **do**
        $Q^{-} \leftarrow \sum_{j=1}^{|L|} D_j - \sum_{veh=1}^{NV_{\psi}} \sum_{j=1}^{NP_{\psi}^{veh}} Q_{\psi,Route_{\psi,j}^{veh}}^{veh}$
        Calculate remaining capacity for each vehicle ($C^{veh} - \sum_{j=1}^{NP_{\psi}^{veh}} Q_{\psi,Route_{\psi,j}^{veh}}^{veh} \forall veh \in NV_{\psi}$)
        Exclude vehicle (veh) with no remaining capacity
        if all vehicles are excluded **then**
            Decide randomly the vehicle (veh) from the remaining vehicles
            Decide randomly the number of ports (NP_{ψ}^{veh}) to be included in the vehicle route ($Route_{\psi}^{veh}$)
            Select randomly NP_{ψ}^{veh} ports and **Add** them to $Route_{\psi}^{veh}$
            Calculate the total quantity ($\sum_{j=1}^{NP_{\psi}^{veh}} Q_{\psi,Route_{\psi,j}^{veh}}^{veh}$) that can be loaded on vehicle (veh) as $\max\{C^{veh}, Q^{-}\}$
            Distribute ($\sum_{j=1}^{NP_{\psi}^{veh}} Q_{\psi,Route_{\psi,j}^{veh}}^{veh}$) randomly among the ports in the route ($Route_{\psi}^{veh}$)
        else
            Select vehicle veh with lowest $C^{veh} - \sum_{j=1}^{NP_{\psi}^{veh}} Q_{\psi,Route_{\psi,j}^{veh}}^{veh}$
            Select randomly ($rnd =$ **randi**($[1\ NP_{\psi}^{veh}]$)) a port ($Route_{\psi,rnd}^{veh}$) such that $Q_{\psi,Route_{\psi,rnd}^{veh}}^{veh} > 0$
            $Q_{\psi,Route_{\psi,rnd}^{veh}}^{veh} \leftarrow Q_{\psi,Route_{\psi,rnd}^{veh}}^{veh} + \min\{C^{veh} - \sum_{j=1}^{NP_{\psi}^{veh}} Q_{\psi,Route_{\psi,j}^{veh}}^{veh}, Q^{-}\}$
        end if
    end while
end while
return Individual chromosomes $Route_{\psi},\ Q_{\psi}\ NP_{\psi},\ NV_{\psi}$

C.4 Fix individual port demand subroutine

Algorithm 3 calls the **Fix Individual Port Demand** subroutine, described in Algorithm 6, in case of any violation in Constraint (30). The algorithm now relies on unloading quantities and transporting them to other ports by using other vehicles in addition to other possible decisions to fix any violation. Let us note that any change performed by this algorithm does not affect the vehicle's capacity (Constraint (31)) or the total demand (Constraint (30)). For each port with an excess quantity, the algorithm first compares the vehicles used on the chromosome with all vehicles and creates a ζ list of unused vehicles.

For the remaining unused vehicles, the algorithm selects a vehicle visiting the port (veh). It then adds a new vehicle (veh$'$) to the solution chromosome and identifies ports with a shortage to the route. The algorithm calculates the quantity to be unloaded from vehicle veh and loaded on vehicle veh$'$ as the minimum between the quantity loaded on veh, the capacity of veh$'$ and the total excess quantity. Then, this quantity is distributed over the newly added ports to the route of vehicle veh$'$. If there are no remaining unused vehicles, the algorithm attempts to redistribute the quantities loaded on a vehicle from the excess ports to the shortage ports. First, the algorithm identifies ports with a shortage ($\mathcal{L}_-$). Then, for each port in ($\mathcal{L}_-$), it creates a list ($\mathcal{W}^{++}$) containing vehicles with the port in their routes and has available capacity. One vehicle is selected, and the quantity loaded to the port is increased such that the vehicle capacity is not exceeded. If $\mathcal{W}^{++}$ is empty, the algorithm chooses a vehicle with an available capacity, adds the port randomly to its route, and moves to it a certain load such that the vehicle capacity is not exceeded. In both the nonempty and empty $\mathcal{W}^{++}$ sets, the loaded quantity was recorded (Q^{--}). An equivalent quantity is removed from ports with excess in $\mathcal{L}_+$. Let us note that calling Algorithm 6 means that the total demand is satisfied, so the excess amount equals the shortage amount. Thus, the algorithm terminates if no excess demand remains. We also start balancing individual port demand by adding more vehicles, although balancing quantities within existing vehicles is possible as a first step. The addition allows the model to consider unloading at one port and loading when using other vehicles, which is a necessary feature of the problem. The algorithm then attempts to reduce the number of vehicles used during the modification step.

Algorithm 6 Fix individual port demand

Input: Q_ψ, UQ_ψ, NV_ψ, NP_ψ, $Route_\psi$, C, D, L
Output: Q_ψ, UQ_ψ, NV_ψ, NP_ψ, $Route_\psi$
for $j \in L$ **do**
  while $\sum^{NV_\psi}_{\substack{veh=1:\\ j\in Route^{veh}_\psi}} Q^{veh}_{\psi,j} - \sum^{NV_\psi}_{\substack{veh=1:\\ j\in Route^{veh}_\psi}} UQ^{veh}_{\psi,j} > D_j$ **do**
    Identify unused vehicles and create ζ list
    if $\zeta \neq \phi$ **then**
      Identify vehicles with port j in their routes, create $\mathcal{W}^+$ list
      Select randomly a vehicle (veh) from $\mathcal{W}^+$ where excess quantity are unloaded at port j
      Select randomly a vehicle (veh') from ζ
      Calculate total quantity to be loaded on vehicle veh' as $Q^+ = \min\left\{C^{veh'}, \min\left\{\left(\sum^{NV_\psi}_{\substack{veh''=1:\\ j\in Route^{veh''}_\psi}} Q^{veh''}_{\psi,j} - \sum^{NV_\psi}_{\substack{veh''=1:\\ j\in Route^{veh''}_\psi}} UQ^{veh''}_{\psi,j} - D_j\right), Q^{veh}_{\psi,j}\right\}\right\}$
      Identify ports with shortage in demand and create $\mathcal{L}^-$
      Distribute Q^+ randomly on ports within $\mathcal{L}^-$
      Add the used ports from $\mathcal{L}^-$ to the vehicle's route $Route^{veh'}_\psi$, such that $Q^+ = \sum_{j''\in\ Route^{veh'}_\psi} Q^{veh'}_{\psi,j''}$
      Update $UQ^{veh}_{\psi,j} \leftarrow UQ^{veh}_{\psi,j} + Q^+$
    else
      Identify ports with shortage in demand and create $\mathcal{L}^-$
      Identify the excess amount $Q^+ = \sum^{NV_\psi}_{\substack{veh=1:\\ j\in Route^{veh}_\psi}} Q^{veh}_{\psi,j} - \sum^{NV_\psi}_{\substack{veh=1:\\ j\in Route^{veh}_\psi}} UQ^{veh}_{\psi,j} - D_j$
      for $j' \in \mathcal{L}^-$ **do**
        Calculate $Q^- = D_{j'} - \left(\sum^{NV_\psi}_{\substack{veh=1:\\ j'\in Route^{veh}_\psi}} Q^{veh}_{\psi,j'} - \sum^{NV_\psi}_{\substack{veh=1:\\ j'\in Route^{veh}_\psi}} UQ^{veh}_{\psi,j'}\right)$
        Create a list of vehicles ($\mathcal{W}^{++}$) such that $veh' \in \mathcal{W}^{++}$ if $j' \in Route^{veh'}_\psi$ and $C^{veh'} > \sum^{NP^{veh'}_\psi}_{j''=1} Q^{veh'}_{\psi,j''}$
        if $\mathcal{W}^{++} \neq \phi$ **then**
          Select a vehicle $veh' \in \mathcal{W}^{++}$
          Set $Q^{--} = \min\left\{C^{veh'} - \sum^{NP^{veh'}_\psi}_{j''=1} Q^{veh'}_{\psi,j''}, Q^-\right\}$
          Update $Q^{veh'}_{\psi,j'} \leftarrow Q^{veh'}_{\psi,j'} + Q^{--}$
        else
          Create a list of vehicles ($\mathcal{W}^+$) such that $veh' \in \mathcal{W}^{++}$ if $C^{veh'} > \sum^{NP^{veh'}_\psi}_{j''=1} Q^{veh'}_{\psi,j''}$
          if $\mathcal{W}^+ \neq \phi$ **then**

Algorithm 6 Fix individual port demand (continued)

Select a vehicle $veh' \in \mathcal{W}^+$
Add port j' to $Route_{\psi}^{veh'}$
Set $Q^{--} = \min\left\{C^{veh'} - \sum_{j''=1}^{NP_{\psi}^{veh'}} Q_{\psi,j''}^{veh'}, Q^{-}\right\}$
Assign $Q_{\psi,j'}^{veh'} \leftarrow Q_{\psi,j'}^{veh'} + Q^{--}$
end if
end if
Identify ports with excess in demand and create $\mathcal{L}^+$
Calculate the excess amount of each port in $\mathcal{L}^+$ as $Q_j^+ = \left(\sum_{\substack{veh=1:\\ j\in Route_{\psi}^{veh}}}^{NV_{\psi}} Q_{\psi,j}^{veh} - \sum_{\substack{veh=1:\\ j\in Route_{\psi}^{veh}}}^{NV_{\psi}} UQ_{\psi,j}^{veh}\right) - D_j$
Select ports such that $\sum_{j\in\mathcal{L}^+} Q_j^+ \geq Q^{--}$ and remove Q^{--} from the selected ports
end for
end if
end while
end for
return Individual chromosomes: Q_{ψ}, UQ_{ψ}, NV_{ψ}, NP_{ψ}, $Route_{\psi}$

Appendix D Heuristic chromosomes and operators

D.1 Chromosome structure

A potential solution in the proposed algorithm consists of four components: vehicle information, route sequence and quantity delivered and transshipment details. The first two are stored in the "route chromosome", and the others are stored in the "quantity chromosome." As a data preparation step, vehicles (inland and trucks) are numbered starting from 1. The depot and ports are also numbered, where 1 is assigned to the depot, 2 is assigned to the first customer/port and so on. Figure D2 illustrates an example of a feasible solution. The route chromosome shows that the individual uses three vehicles (5, 1 and 3). Once the vehicle number is known, its type (inland or truck), capacity and other parameters can be easily determined. Vehicle 5 starts from 2 and visits 5 "Customer/Port 4" and 9 "Customer/Port 8," implying that it carries a transshipment quantity as it starts from Customer 1. The quantity chromosome shows that a quantity of 150 is carried by this vehicle at 2 "Customer 1," where 100 is delivered to 5 and 50 is delivered to 9. Vehicle 1 starts from 1 "Depot" (Route chromosome) and carries a quantity of 550. It then visits 3 "Customer 2" and delivers 100, 2 "Customer 1" delivers 70 and unloads 150 as a transshipment. After that, it visits 6 "Customer 5" to deliver 150, 4 "Customer 3" to deliver 50 and 7 "Customer 6" to deliver 30.

Route chromosome

Vehicle type	Depot	Route				
5	2	5	9			
1	1	3	2	6	4	7
3	1	4	6	7	8	

Quantity chromosome

Vehicle type	Total Quantity loaded	Source	Quantity delivered to customers (Q) and transhipment (UQ)							
				2	3	4	5	6	7	8	9
5	150	2	Q				100				50
			UQ								
1	550	1	Q	70	100	50		150	30		
			UQ	150							
3	340	1	Q			100		150	30	60	
			UQ								

Fig. D2: Chromosome structure

D.2 Route operators

Operators 2–7 are designed to modify the path of one randomly selected vehicle (operators 2, 4 and 6) or multiple randomly selected vehicles (operators 3,5 and 7), where the number of vehicles is assigned randomly. The Flip operator must identify two ports randomly and then flip between those ports (e.g., 3,2,6,4 becomes 4,6,2,3, assuming that the two chosen ports are 3 and 4), as shown in Figure D3. The swap operator must choose two ports randomly and then exchange their visit sequence without affecting the visit sequence of ports between the chosen ports (e.g., 3, 2, 6, and 4 become 4, 2, 6, and 3, assuming that the two chosen ports are 3 and 4), as shown in Figure D3 for one vehicle (Operator 4) and multiple vehicles (Operator 5). The slide operator also requires choosing two ports randomly. It then brings the second selected port to the location of the first port and slides (pushes) the first port and ports between the first and last ports to the right (e.g., 3,2,6,4 becomes 4,3,2,6 assuming that the first randomly selected port is 3 and the second is 4). Figure D3 shows the slide operator in the case of one vehicle and multiple vehicles.

D.3 Starting point operator

Operator 8 tries to reduce transshipment by selecting a random vehicle that does not start from the depot then changes its starting point to be the depot (e.g., vehicle 5 in Figure D4: depot changed from 2 "customer location" to 1 "original depot"). This process involves reducing the transshipment quantity (UQ) of another vehicle (UQ = 150 of Vehicle 1 in Figure D4) by the total quantity delivered using that randomly selected vehicle (vehicle 5). In Figure D4, as vehicle 5 starts from the depot, its delivered quantity to ports 5 and 9 ($Q = 150$) is removed from the transshipment quantity of Vehicle 1 (UQ = 0), resulting in no transshipment. In addition, the total loaded quantity on Vehicle 1 must be adjusted because this vehicle no longer transships (550˘150 = 400). Let us note that these changes do not affect the vehicle capacity constraints as we never increase the loaded quantities on any vehicle and that the

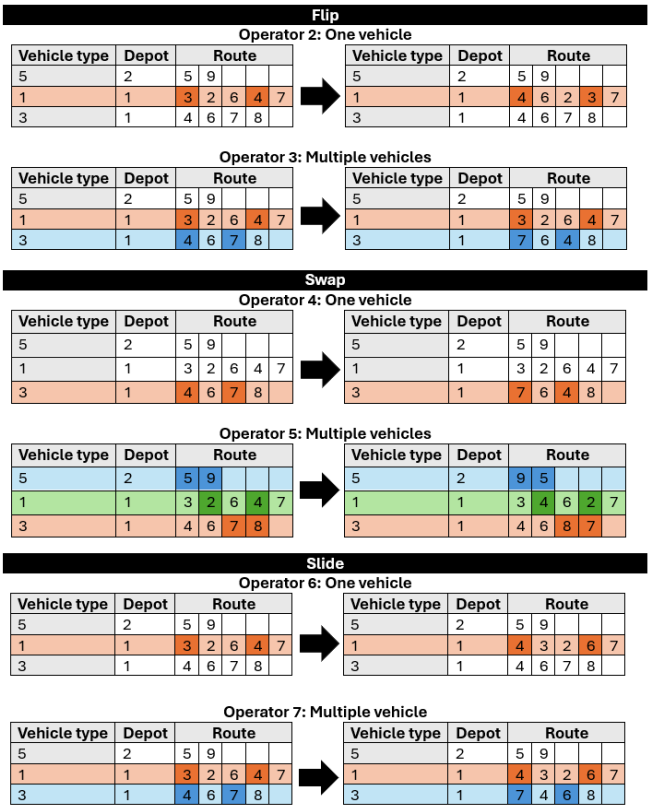

Fig. D3: Route operators

demand constraint is always fulfilled as we do not reduce the quantity delivered to ports (all individuals are generated so that they fulfill the demand). We do not provide an operator that changes the starting point to include a transshipment, as this requires increasing the total quantity loaded on a vehicle, which requires capacity verification. Otherwise, it can lead to capacity violation. However, this aspect is covered in the initial population generation when all the required checks are conducted.

D.4 Vehicle type operators

Operators 9 and 10 change the vehicle type. Operator 9 tries to lower capacity by switching to a vehicle with lower capacity to enhance the utilization. The operator chooses one vehicle randomly, checks its total loaded quantity and tries to find an unused vehicle with lower capacity. In contrast, Operator 10 changes the current vehicle with another random vehicle (lower or higher capacity) with the restriction that the chosen vehicle must be able to transport all assigned quantities (no capacity violation). This operator can explore different possibilities, such as moving to larger vehicles that might have more allocated quantities in the next generation through other operators, such as 15 and 16. Figure D5 shows that Vehicle 1, which is randomly selected, can

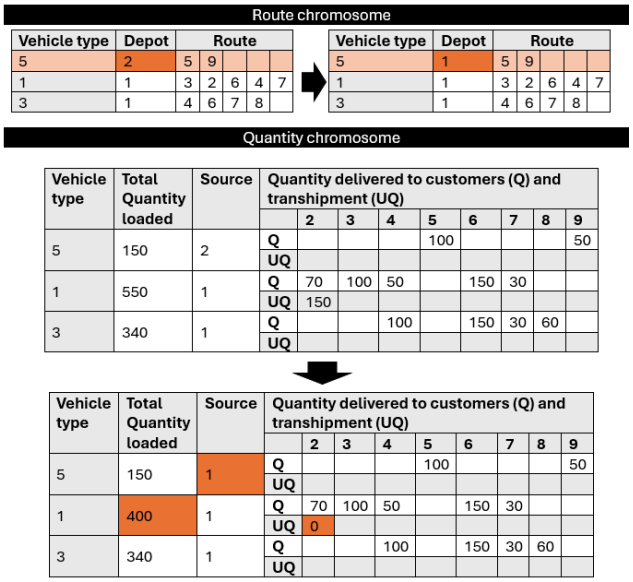

Fig. D4: Starting point operator

be changed to Vehicle 4, which is smaller than Vehicle 1 in this hypothetical example but can accommodate the loaded quantity (Operator 9) or change to a random vehicle that can carry at least the loaded quantities.

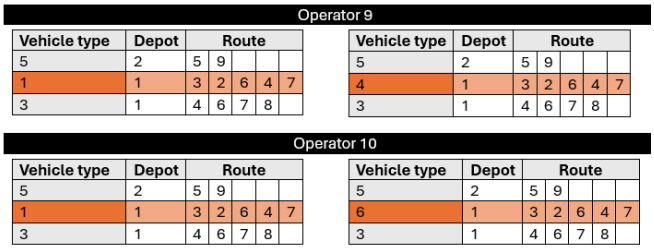

Fig. D5: Vehicle type operators

D.5 Quantity exchange operators

Operator 11 selects two vehicles that start from a depot randomly and identifies one port visited by each, named a and b, where a is the selected port currently served by the first vehicle and b is the selected port currently served by the second vehicle. Then, it calculates the remaining capacity if the current port is replaced with the other port (from the other vehicle) as $C-(\sum Q-Q_a+Q_b)$ for Vehicle 1 and $C-(\sum Q-Q_b+Q_a)$ for Vehicle 2. If the remaining capacity is nonnegative for both vehicles, exchange occurs,

where the quantity Q_a is served by Vehicle 2 and Q_b is served by Vehicle 1. Let us note that if the original route of Vehicle 1 includes port b, then Q_b is added to the existing quantity, and if it originally does not serve this port, then it is added to the route at a random location. The same concept applies to Vehicle 2. Figure D6 illustrates how this operator works. In this figure, Vehicles 1 and 3 are chosen randomly, and then Port 3 on Vehicle 1 and Port 4 on Vehicle 3 are chosen randomly. Exchanging the quantities does not violate the capacity constraint; thus, it is permitted. Consequently, Vehicle 1 delivers 150 to Port 4 (previously, it was assigned to deliver 50), and Vehicle 3 delivers 100 to Port 3. Let us note that Port 4 is removed from Vehicle 3 and that Port 3 is removed from Vehicle 1 then added to Vehicle 3 since it was not served before. Operator 12 is similar to Operator 11; however, instead of doing one change in each generation (iteration), it tries to exchange more than one port between the two vehicles, where the number of exchanges is decided randomly based on the smallest number of ports visited by the vehicles.

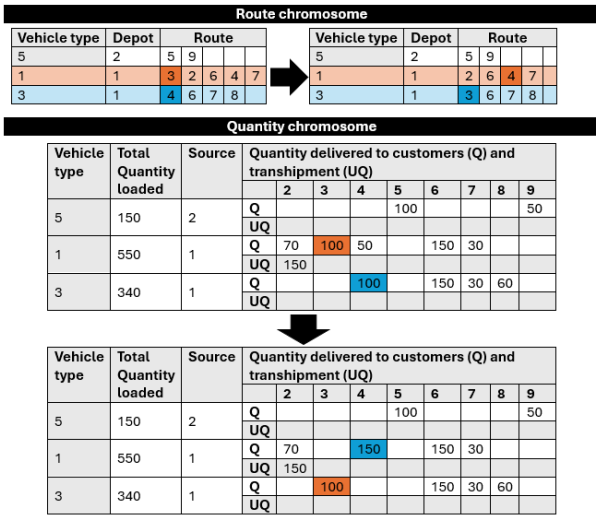

Fig. D6: Illustration of Operator 11

Operator 13 considers exchanging unique ports between two vehicles (Figure D7). Operator 13 randomly identifies two vehicles (Vehicles 1 and 3 in Figure D7). Then, it checks the route of each vehicle and identifies unique ports on each vehicle (i.e., ports not visited by the other vehicle). In Figure D7, the unique ports are 2 and 3 for Vehicle 1 and 8 for Vehicle 3. It then selects one port served by the first vehicle and tries to exchange it with one or more unique ports served by the second vehicle based on the remaining capacity. In Figure D7, Port 3 served by the first vehicle (Vehicle 1) is chosen as a unique port, and since the second vehicle (Vehicle 3) has only one unique port (port 8), the operator tries to exchange 3 and 8. First, the remaining capacity of Vehicle 1 and the quantity delivered to port are calculated as $(C - \sum Q - Q_3)$, which represents the allowable exchange limit of Vehicle 1 after removing Port 3. Then, for

the second vehicle (Vehicle 3), the algorithm searches for an equivalent exchange (i.e., a unique port with a quantity close to the allowable exchange limit of Vehicle 1). If no port exists with a matching quantity, the algorithm searches for multiple unique ports not exceeding the allowable exchange limit of Vehicle 1. Then, it swaps the quantities between the two vehicles and adds the new ports to the vehicles' routes if capacity limit allows this exchange. In Figure D7, the second vehicle (Vehicle 3) has only one unique port (Port 8). Thus, it checks the remaining capacity as $C - \sum Q - Q_8$ and compares it with the quantity of Port 3. The exchange of Ports 3 and 8 is permitted since the capacity is not violated. Operator 14 has a similar functionality to Operator 13, except that it tries to swap ports between Vehicle 1 and multiple other vehicles, where the number of vehicles involved is chosen randomly based on the number of vehicles involved in the service.

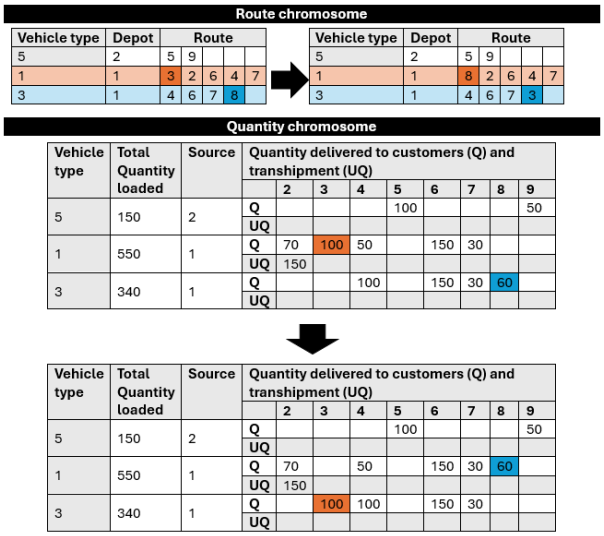

Fig. D7: Illustration of Operator 13

D.6 Quantity transfer operators

Operators 15–18 are unidirectional quantity movement operators. Operator 15, as shown in Figure D8, identifies vehicles that start from the depot and are not fully utilized (i.e., have remaining capacities) and selects two random vehicles. It identifies the vehicle with the highest utilization (smallest remaining capacity) to receive quantities, called the receiving vehicle, and the vehicle with the lowest utilization, named the sending vehicle. In Figure D8, the receiving and sending vehicles are assumed to be Vehicles 1 and 3, respectively. It calculates the remaining capacity of the receiving vehicle and then randomly selects a subset of the ports served by the sending vehicle. Figure D8 shows an example of a subset of one port (Port 7). It then transfers quantities from each chosen port on the sending vehicle (Port 7 in this example) as long as

the transferable quantities are within the vehicle's remaining capacity. The transfer process stops when either the remaining capacity reaches zero or a random number of ports is reached. Let us note that if the receiving vehicle does not originally visit a certain port, it is then added to the route randomly. We note also that this operator does not necessarily result in a fully utilized receiving vehicle (e.g., if the total quantity transferred due to the number of selected ports is less than the remaining capacity). The route sequence chromosome is updated accordingly. Operator 16 follows the same concept as Operator 15 but ensures that the receiving vehicle is fully utilized by allowing more than one vehicle to be a sending vehicle. In the case where the receiving vehicle receives all quantities transported by a sending vehicle, the sending vehicle is removed from the service.

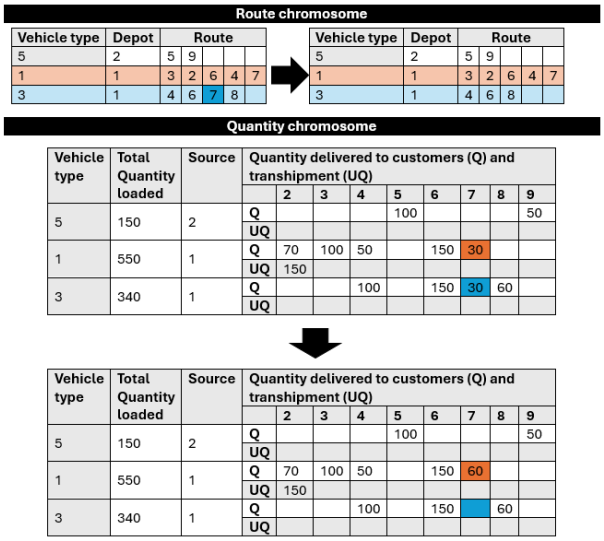

Fig. D8: Illustration of Operator 15

Operator 17, shown in Figure D9, represents a simplified version of Operator 11, where the quantity movement occurs in one direction. That is, one port served by the sending vehicle is chosen randomly (Port 3 of Vehicle 1), and the possibility of moving its quantity to the receiving vehicle (Vehicle 3 in Figure D9) is checked. If the remaining capacity is nonnegative, then the port is moved to the receiving vehicle. Operator 18 is the multiple port transfer version of Operator 17.

Appendix E Case study data

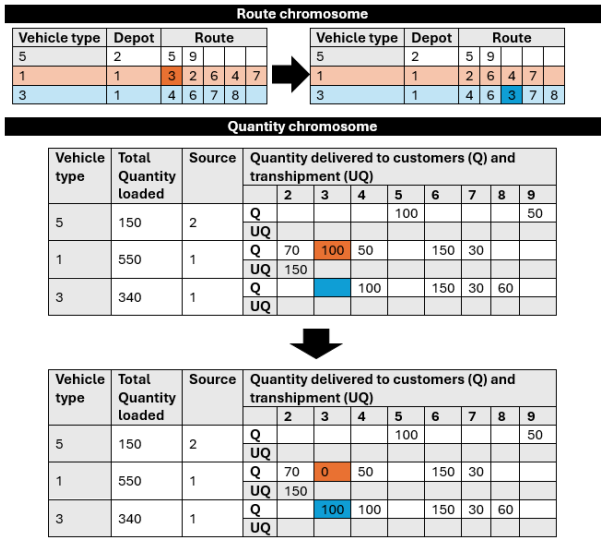

Fig. D9: Illustration of Operator 17

Table E1: Input data for the different transportation modes

Notation	Inland waterway transportation	Truck	Unit
$\alpha^{k,m}$	58.88 – 103.45	0.1506	[€/h], [€/km]
$C^{k,m}$	900 – 2000	26	[t]
$\beta^{k,m}$	37.52 – 44.95	19.33	[€/h]
$n^{k,m}$	2 – 2.43	–	–
$d_{i,j}^{k,m}$	see Table E5	see Table E6	[km]
$q_{i,j}$	see Table E2	–	–
h	1	–	[h]
τ	0.67	–	[h]
η	230	–	[t/h]
$\mu^{k,m}$	20.36 – 24.25	0.3208	[€/km]
p	0.44	–	[€/t]
$\epsilon^{k,m}$	3,25	2	[€/t]
$\gamma^{k,m}$	2,30	3,25	[€/t]
$s^{k,m}$	10	65	[km/h]
$\Pi^{k,m}$	–	0.08	[€/h]
$\urcorner^{k,m}$	–	13.54	[€/h]
$\mathbb{T}^{k,m}$	–	0.155	[€/km]
$\kappa_{i,j}^{k,m}$	0,15	see Table E4	–
z	3.6		
$r^{k,m}$	0,45	$f_{i,j}^{k,m}/C^{k,m}$	–
ρ	23,2	23,2	[g/MJ]
ϕ	0,03– 1,4	0,03 – 1,4	[g/km]
ξ	0,0957	0,277	[g/MJ]
$\omega^{k,m}$	152 – 181	–	[kW]
$\chi^{k,m}$	–	–	[g]
$E^{k,m}$	–	10,9	[MJ/km]

Table E2: Matrix of the number of locks between port i and j for the single inland waterway transportation model

Ports	0	1	2	3	4	5	6	7	8	9	10	11	12	13	14	15
0	0	1	2	7	4	1	1	2	2	4	4	4	3	3	3	6
1	1	0	1	6	3	0	0	1	1	3	3	3	2	2	2	5
2	2	1	0	7	4	1	1	2	2	4	4	4	3	3	3	6
3	7	6	7	0	3	6	6	7	7	2	2	2	3	3	3	0
4	4	3	4	3	0	3	3	4	4	6	6	6	5	5	5	8
5	1	0	1	6	3	0	0	1	1	3	3	3	2	2	2	5
6	1	0	1	6	3	0	0	1	1	3	3	3	2	2	2	5
7	2	1	2	7	4	1	1	0	0	4	4	4	3	3	3	6
8	2	1	2	7	4	1	1	0	0	4	4	4	3	3	3	6
9	4	3	4	2	6	3	3	4	4	0	0	0	1	1	1	2
10	4	3	4	2	6	3	3	4	4	0	0	0	1	1	1	2
11	4	3	4	2	6	3	3	4	4	0	0	0	1	1	1	2
12	3	2	3	3	5	2	2	3	3	1	1	1	0	0	0	3
13	3	2	3	3	5	2	2	3	3	1	1	1	0	0	0	3
14	3	2	3	3	5	2	2	3	3	1	1	1	0	0	0	3
15	6	5	6	0	8	5	5	6	6	2	2	2	3	3	3	0

Table E3: Infrastructure failure scenarios

Scenario	Infrastructure failure	Accessibility	Scenario	Infrastructure failure	Accessibility
1	Meiderich	yes	7	Hamm	no
	Oberhausen	yes	8	Münster	no
2	Gelsenkirchen	yes	9	Dortmund-Ems-Kanal	no
3	Wanne Eickel Herne Ost	yes			
4	Henrichenburg	no	10	Datteln-Hamm-Kanal	no
5	Datteln		11	Rhein-Herne-Kanal	no
	Ahsen Flaesheim	yes			
6	Dorsten		12	Wesel-Datteln Kanal	no
	Hünxe Friedrichsfeld	yes			

Table E4: Empty percentage for trucks from port i to j

Ports	0	1	2	3	4	5	6	7
0	-	0.38	0.30	0.30	0.38	0.30	0.38	0.30
1	0.38	-	0.38	0.30	0.38	0.38	0.44	0.38
2	0.30	0.38	-	0.38	0.44	0.44	0.44	0.38
3	0.30	0.30	0.38	-	0.38	0.38	0.38	0.30
4	0.38	0.38	0.44	0.38	-	0.44	0.38	0.38
5	0.30	0.38	0.44	0.38	0.44	-	0.44	0.44
6	0.38	0.44	0.44	0.38	0.38	0.44	-	0.44
7	0.30	0.38	0.38	0.30	0.38	0.44	0.44	-
8	0.30	0.38	0.38	0.30	0.38	0.44	0.44	0.44
9	0.30	0.38	0.44	0.44	0.44	0.44	0.38	0.38
10	0.30	0.38	0.44	0.44	0.44	0.44	0.38	0.38
11	0.30	0.38	0.44	0.44	0.44	0.44	0.38	0.38
12	0.30	0.38	0.44	0.38	0.44	0.44	0.38	0.38
13	0.30	0.38	0.44	0.44	0.44	0.44	0.38	0.38
14	0.30	0.38	0.44	0.38	0.44	0.44	0.38	0.38
15	0.30	0.38	0.38	0.44	0.44	0.38	0.38	0.30
Ports	8	9	10	11	12	13	14	15
0	0.30	0.30	0.30	0.30	0.30	0.30	0.30	0.30
1	0.38	0.38	0.38	0.38	0.38	0.38	0.38	0.30
2	0.38	0.44	0.44	0.44	0.44	0.44	0.44	0.38
3	0.30	0.44	0.44	0.44	0.38	0.44	0.38	0.44
4	0.38	0.44	0.44	0.44	0.44	0.44	0.44	0.44
5	0.44	0.44	0.44	0.44	0.44	0.44	0.44	0.38
6	0.44	0.38	0.38	0.38	0.44	0.38	0.44	0.38
7	0.44	0.38	0.38	0.38	0.38	0.38	0.38	0.30
8	-	0.38	0.38	0.38	0.38	0.38	0.38	0.30
9	0.38	-	0.44	0.44	0.44	0.44	0.44	0.44
10	0.38	0.44	-	0.44	0.44	0.44	0.44	0.44
11	0.38	0.44	0.44	-	0.44	0.44	0.44	0.44
12	0.38	0.44	0.44	0.44	-	0.44	0.44	0.44
13	0.38	0.44	0.44	0.44	0.44	-	0.44	0.44
14	0.38	0.44	0.44	0.44	0.44	0.44	-	0.44
15	0.30	0.44	0.44	0.44	0.44	0.44	0.44	-

Table E5: Distance matrix for inland waterway transportation from port i to j

Ports	0	1	2	3	4	5	6	7
0	0	40.15	104.74	144.39	107.29	98.33	110.35	131.92
1	40.15	0	64.58	104.24	67.14	58.18	70.20	91.77
2	104.74	64.58	0	78.54	41.43	28.87	40.89	62.46
3	144.39	104.24	78.54	0	37.10	72.13	84.15	105.72
4	107.29	67.14	41.43	37.10	0	35.03	47.05	68.62
5	98.33	58.18	28.87	72.13	35.03	0	12.02	33.59
6	110.35	70.20	40.89	84.15	47.05	12.02	0	21.57
7	131.92	91.77	62.46	105.72	68.62	33.59	21.57	0
8	134.41	94.25	64.94	108.21	71.10	36.07	24.06	11.46
9	120.70	80.55	44.47	54.17	57.40	44.84	56.85	78.43
10	120.70	80.55	44.47	54.17	57.40	44.84	56.85	78.43
11	120.70	80.55	44.47	54.17	57.40	44.84	56.85	78.43
12	108.80	68.65	32.57	66.39	45.50	32.94	44.95	66.53
13	112.50	72.35	36.27	62.37	49.20	36.64	48.66	70.23
14	105.86	65.70	29.62	69.02	42.55	29.99	42.01	63.58
15	135.70	95.55	59.47	40.17	72.40	59.83	71.85	93.42
Ports	8	9	10	11	12	13	14	15
0	134.41	120.70	120.70	120.70	108.80	112.50	105.86	135.70
1	94.25	80.55	80.55	80.55	68.65	72.35	65.70	95.55
2	64.94	44.47	44.47	44.47	32.57	36.27	29.62	59.47
3	108.21	54.17	54.17	54.17	66.39	62.37	69.02	40.17
4	71.10	57.40	57.40	57.40	45.50	49.20	42.55	72.40
5	36.07	44.84	44.84	44.84	32.94	36.64	29.99	59.83
6	24.06	56.85	56.85	56.85	44.95	48.66	42.01	71.85
7	11.46	78.43	78.43	78.43	66.53	70.23	63.58	93.42
8	0	80.91	80.91	80.91	69.01	72.71	66.06	95.91
9	80.91	0	0	0	12.22	8.20	14.85	15.00
10	80.91	0	0	0	12.22	8.20	14.85	15.00
11	80.91	0	0	0	12.22	8.20	14.85	15.00
12	69.01	12.22	12.22	12.22	0	4.02	2.94	27.21
13	72.71	8.20	8.20	8.20	4.02	0	6.65	23.19
14	66.06	14.85	14.85	14.85	2.94	6.65	0	29.84
15	95.91	15.00	15.00	15.00	27.21	23.19	29.84	0

Table E6: Distance matrix for trucks from port i to j

Ports	0	1	2	3	4	5	6	7
0	0.00	57.28	115.24	136.53	96.09	102.96	83.63	113.78
1	57.23	0.00	75.09	108.84	55.75	62.80	43.48	73.62
2	121.79	80.36	0.00	76.92	46.99	10.62	45.78	62.97
3	135.66	110.02	77.41	0.00	55.82	77.96	97.69	114.87
4	97.42	56.31	46.76	54.69	0.00	47.30	67.04	84.22
5	104.85	63.42	10.52	76.78	46.85	0.00	13.44	46.03
6	87.29	45.86	23.46	91.43	61.50	13.44	0.00	36.83
7	113.34	71.90	63.90	114.22	84.29	45.21	37.33	0.00
8	114.34	72.90	64.90	115.22	85.29	46.21	38.33	3.05
9	134.29	80.17	40.91	44.16	25.97	48.66	68.40	85.58
10	135.93	81.82	40.79	44.04	27.62	47.12	66.86	84.04
11	134.28	80.17	40.13	43.37	25.97	48.66	68.39	85.57
12	115.08	73.98	28.62	51.46	24.38	36.26	55.99	73.18
13	138.86	81.00	33.66	46.18	23.24	39.99	59.72	76.91
14	114.99	73.89	27.04	51.04	30.51	36.17	55.90	73.08
15	145.67	99.65	59.20	29.93	45.45	67.58	87.32	104.50
Ports	8	9	10	11	12	13	14	15
0	114.77	135.14	136.78	135.14	115.63	121.06	113.89	149.81
1	74.62	79.56	81.20	79.56	75.29	80.72	73.54	108.45
2	63.96	41.33	41.21	40.54	28.57	34.00	26.83	58.38
3	115.86	42.55	43.71	43.04	50.92	48.23	51.65	43.06
4	85.21	25.40	27.05	25.40	30.94	23.06	29.19	48.49
5	47.02	48.35	46.80	46.13	34.17	39.60	32.42	70.58
6	37.83	63.00	61.45	60.79	48.82	54.25	47.08	85.23
7	3.05	85.79	84.24	85.79	71.61	77.04	69.87	108.03
8	0.00	86.79	85.24	86.79	72.61	78.04	70.87	109.02
9	86.57	0.00	2.43	0.79	14.37	11.68	17.08	30.29
10	85.03	2.43	0.00	1.65	14.25	11.56	16.96	30.17
11	86.57	0.79	1.65	0.00	13.58	10.89	16.29	29.50
12	74.17	15.81	15.69	15.02	0.00	5.47	5.90	37.59
13	77.90	10.53	10.41	9.75	5.47	0.00	9.83	32.31
14	74.08	17.46	17.34	16.68	4.71	10.14	0.00	39.24
15	105.49	25.57	25.45	24.78	32.65	29.96	35.36	0.00

References

Almeida, C.P., Gonçalves, R.A., Goldbarg, E.F., Goldbarg, M.C., Delgado, M.R. (2012). An experimental analysis of evolutionary heuristics for the biobjective traveling purchaser problem. *Annals of Operations Research*, *199*(1), 305–341,

Alsharqawi, M., Abu Dabous, S., Zayed, T., Hamdan, S. (2021). Budget optimization of concrete bridge decks under performance-based contract settings. *Journal of Construction Engineering and Management*, *147*(6), 04021040,

Alumur, S.A., Kara, B.Y., Karasan, O.E. (2012). Multimodal hub location and hub network design. *Omega*, *40*(6), 927–939,

Annouch, A., Bellabdaoui, A., Minkhar, J. (2016). Split delivery and pickup vehicle routing problem with two-dimensional loading constraints. *2016 11th international conference on intelligent systems: Theories and applications (sita)* (pp. 1–6).

Arora, S., & Barak, B. (2009). *Computational complexity: a modern approach*. Cambridge University Press.

Assadipour, G., Ke, G.Y., Verma, M. (2016). A toll-based bi-level programming approach to managing hazardous materials shipments over an intermodal transportation network. *Transportation Research Part D: Transport and Environment*, *47*, 208-221,

Bernardino, R., & Paias, A. (2018). Solving the family traveling salesman problem. *European Journal of Operational Research*, *267*(2), 453-466,

Bernardino, R., & Paias, A. (2021). Heuristic approaches for the family traveling salesman problem. *International Transactions in Operational Research*, *28*(1), 262-295,

Borthen, T., Loennechen, H., Wang, X., Fagerholt, K., Vidal, T. (2018). A genetic search-based heuristic for a fleet size and periodic routing problem with application to offshore supply planning. *EURO Journal on Transportation and Logistics*, *7*(2), 121-150,

Bożejko, W., & Wodecki, M. (2009). Solving permutational routing problems by population-based metaheuristics. *Computers & Industrial Engineering*, *57*(1),

269-276,

Cariou, P., Cheaitou, A., Larbi, R., Hamdan, S. (2018). Liner shipping network design with emission control areas: A genetic algorithm-based approach. *Transportation Research Part D: Transport and Environment*, *63*, 604–621,

Cheaitou, A., Hamdan, S., Larbi, R. (2021). Liner shipping network design with sensitive demand. *Maritime Business Review*, *6*(3), 293–313,

Cheaitou, A., Hamdan, S., Larbi, R., Alsyouf, I. (2021). Sustainable traveling purchaser problem with speed optimization. *International Journal of Sustainable Transportation*, *15*(8), 621–640,

Cheng, Y. (2012). The method to select the transport path based on the multimodal cost. *Transport*, *27*(2), 143–148,

Créput, J.-C., Hajjam, A., Koukam, A., Kuhn, O. (2012). Self-organizing maps in population based metaheuristic to the dynamic vehicle routing problem. *Journal of combinatorial optimization*, *24*, 437–458,

Dehghani, M., Esmaeilian, M., Tavakkoli-Moghaddam, R. (2013). Employing fuzzy anp for green supplier selection and order allocations: a case study. *International Journal of Economy, Management and Social Sciences*, *2*(8), 565–575,

Demir, E., Burgholzer, W., Hrušovskỳ, M., Arıkan, E., Jammernegg, W., Van Woensel, T. (2016). A green intermodal service network design problem with travel time uncertainty. *Transportation Research Part B: Methodological*, *93*, 789–807,

Dong, X., & Cai, Y. (2019). A novel genetic algorithm for large scale colored balanced traveling salesman problem. *Future Generation Computer Systems*, *95*, 727-742,

Dong, X., Lin, Q., Shen, F., Guo, Q., Li, Q. (2023). A novel hybrid simulated annealing algorithm for colored bottleneck traveling salesman problem. *Swarm and Evolutionary Computation*, *83*, 101406,

Dulebenets, M.A. (2018). A comprehensive multi-objective optimization model for the vessel scheduling problem in liner shipping. *International Journal of Production*

Economics, *196*, 293-318,

Elbert, R., Müller, J.P., Rentschler, J. (2020). Tactical network planning and design in multimodal transportation – a systematic literature review. *Research in Transportation Business & Management*, *35*, 100462,

El-Dean, R.A.-H.Z. (2008). A tabu search approach for solving the travelling purchase problem. *Proceedings of the international conference on informatics and system, infos2008* (pp. 24–30).

Fazayeli, S., Eydi, A., Kamalabadi, I.N. (2018). Location-routing problem in multimodal transportation network with time windows and fuzzy demands: Presenting a two-part genetic algorithm. *Computers & Industrial Engineering*, *119*, 233–246,

Federal Ministry of Transport and Digital Infrastructure (2016). *Entwicklung eines Modells zur Berechnung von modalen Verlagerungen im Güterverkehr für die Ableitung konsistenter Bewertungsansätze für die Bundesverkehrswegeplanung* (Tech. Rep. No. FE 96.1002/2012). Bundesministerium für Verkehr und digitale Infrastruktur.

Federal Ministry of Transport and Digital Infrastructure (2019). *Inland Waterway Transport Masterplan.* Berlin.

Federal Office of Statistics (2019). *Freight Transport Statistics in Inland Waterway Transport.*

Fonseca, C.M., & Fleming, P.J. (1998). Multiobjective optimization and multiple constraint handling with evolutionary algorithms. ii. application example. *IEEE Transactions on systems, man, and cybernetics-Part A: Systems and humans*, *28*(1), 38–47,

Garey, M.R., & Johnson, D.S. (1979). *Computers and intractability: A guide to the theory of np-completeness.* New Yord: Freeman.

Gast, J., Wehrle, R., Wiens, M., Schultmann, F. (2020). Impact of notification time on risk mitigation in inland waterway transport. *Data science and innovation in supply chain management: How data transforms the value chain. proceedings of the hamburg international conference of logistics (hicl), vol. 29* (pp. 247–278).

Ghane-Kanafi, A., & Khorram, E. (2015). A new scalarization method for finding the efficient frontier in non-convex multi-objective problems. *Applied Mathematical Modelling*, *39*(23), 7483-7498,

Ghiani, G., Laporte, G., Musmanno, R. (2004). *Introduction to logistics systems planning and control*. John Wiley & Sons.

Goldbarg, M.C., Bagi, L.B., Goldbarg, E.F.G. (2009). Transgenetic algorithm for the traveling purchaser problem. *European Journal of Operational Research*, *199*(1), 36–45,

Govindan, K., Jafarian, A., Khodaverdi, R., Devika, K. (2014). Two-echelon multiple-vehicle location–routing problem with time windows for optimization of sustainable supply chain network of perishable food. *International Journal of Production Economics*, *152*, 9–28,

Gutin, G., & Punnen, A.P. (2006). *The traveling salesman problem and its variations* (Vol. 12). Springer Science & Business Media.

Hadjicharalambous, G., Pop, P., Pyrga, E., Tsaggouris, G., Zaroliagis, C. (2007). The railway traveling salesman problem. F. Geraets, L. Kroon, A. Schoebel, D. Wagner, & C.D. Zaroliagis (Eds.), *Algorithmic methods for railway optimization* (pp. 264–275). Berlin, Heidelberg: Springer Berlin Heidelberg.

Hamdan, S., Cheaitou, A., Shikhli, A., Alsyouf, I. (2023). Comprehensive quantity discount model for dynamic green supplier selection and order allocation. *Computers & Operations Research*, *160*, 106372,

Hao, C., & Yue, Y. (2016). Optimization on combination of transport routes and modes on dynamic programming for a container multimodal transport system. *Procedia Engineering*, *137*(1), 382–390,

He, Z., Navneet, K., van Dam, W., Van Mieghem, P. (2021). Robustness assessment of multimodal freight transport networks. *Reliability Engineering & System Safety*, *207*, 107315,

Ilavarasi, K., & Joseph, K.S. (2014). Variants of travelling salesman problem: A survey. *International conference on information communication and embedded systems (icices2014)* (p. 1-7).

Infante, D., Paletta, G., Vocaturo, F. (2009). A ship-truck intermodal transportation problem. *Maritime Economics & Logistics*, *11*(3), 247–259,

Institut für Energie- und Umweltforschung Heidelberg gGmbH (2023). *Ecological Transport Information Tool for Worldwide Transports.* EcoTransIT World Initiative (EWI).

ISO (2019). *Greenhouse gases — quantification and reporting of greenhouse gas emissions of transport operations.* https://www.iso.org/standard/78864.html. Accessed September 16, 2020.

Jafarzadeh, H., Moradinasab, N., Elyasi, M. (2017). An enhanced genetic algorithm for the generalized traveling salesman problem. *Engineering, Technology & Applied Science Research*, *7*(6), 2260–2265,

Janic, M. (2007). Modelling the full costs of an intermodal and road freight transport network. *Transportation Research Part D: Transport and Environment*, *12*(1), 33–44,

Jeong, H.Y., Song, B.D., Lee, S. (2019). Truck-drone hybrid delivery routing: Payload-energy dependency and no-fly zones. *International Journal of Production Economics*, *214*, 220–233,

Jungnickel, D. (1999). A hard problem: The tsp. In *Graphs, networks and algorithms* (pp. 423–469). Berlin, Heidelberg: Springer Berlin Heidelberg.

Kaewfak, K., Ammarapala, V., Huynh, V.-N. (2021). Multi-objective optimization of freight route choices in multimodal transportation. *International Journal of Computational Intelligence Systems*, *14*(1), 794–807,

Lee, C.-G., Epelman, M.A., White III, C.C., Bozer, Y.A. (2006). A shortest path approach to the multiple-vehicle routing problem with split pick-ups. *Transportation research part B: Methodological*, *40*(4), 265–284,

Liu, J., Mirchandani, P., Zhou, X. (2020). Integrated vehicle assignment and routing for system-optimal shared mobility planning with endogenous road congestion. *Transportation Research Part C: Emerging Technologies*, *117*, 102675,

Liu, S. (2013). A hybrid population heuristic for the heterogeneous vehicle routing problems. *Transportation Research Part E: Logistics and Transportation Review*, *54*, 67-78,

Londoño, A., González, W., Giraldo, O., Escobar, J. (2024). A hybrid heuristic approach for the multi-objective multi depot vehicle routing problem. *International Journal of Industrial Engineering Computations*, *15*(1), 337–354,

Mahmoudinazlou, S., & Kwon, C. (2024). A hybrid genetic algorithm for the min–max multiple traveling salesman problem. *Computers & Operations Research*, *162*, 106455,

Manerba, D., & Mansini, R. (2012). The capacitated traveling purchaser problem with total quantity discount. *Proceedings of odysseus 2012 conference* (p. 42).

Manerba, D., Mansini, R., Riera-Ledesma, J. (2017). The Traveling Purchaser Problem and its variants. *European Journal of Operational Research*, *259*(1), 1–18,

Mansini, R., Pelizzari, M., Saccomandi, R. (2005). An effective tabu search algorithm for the capacitated traveling purchaser problem. *Technical report tr2005-10-49* (pp. 10–49). DEA, University of Brescia.

Marler, R.T., & Arora, J.S. (2004). Survey of multi-objective optimization methods for engineering. *Structural and multidisciplinary optimization*, *26*(6), 369–395,

Miller, C.E., Tucker, A.W., Zemlin, R.A. (1960). Integer programming formulation of traveling salesman problems. *Journal of the ACM (JACM)*, *7*(4), 326–329,

Min, H. (1989). The multiple vehicle routing problem with simultaneous delivery and pick-up points. *Transportation Research Part A: General*, *23*(5), 377–386,

Moccia, L., Cordeau, J.-F., Laporte, G., Ropke, S., Valentini, M.P. (2011). Modeling and solving a multimodal transportation problem with flexible-time and scheduled services. *Networks*, *57*(1), 53–68,

Molina, J.C., Eguia, I., Racero, J., Guerrero, F. (2014). Multi-objective vehicle routing problem with cost and emission functions. *Procedia-Social and Behavioral Sciences*, *160*, 254–263,

Nearchou, A.C. (2010). Scheduling with controllable processing times and compression costs using population-based heuristics. *International Journal of Production Research*, *48*(23), 7043–7062,

Nitsenko, V., Kotenko, S., Hanzhurenko, I., Mardani, A., Stashkevych, I., Karakai, M. (2020). Mathematical modeling of multimodal transportation risks. *International conference on soft computing and data mining* (pp. 439–447).

Pop, P.C., Cosma, O., Sabo, C., Sitar, C.P. (2024). A comprehensive survey on the generalized traveling salesman problem. *European Journal of Operational Research*, *314* (3), 819-835,

Przystupa, K., Qin, Z., Zabolotnii, S., Pohrebennyk, V., Mogilei, S., Zhongju, C., Gil, L. (2021). Constructing reference plans of two-criteria multimodal transport problem. *Transport and Telecommunication Journal*, *2*, ,

Qu, Y., Bektaş, T., Bennell, J. (2016). Sustainability si: multimode multicommodity network design model for intermodal freight transportation with transfer and emission costs. *Networks and Spatial Economics*, *16* (1), 303–329,

Rao, M. (1980). A note on the multiple traveling salesmen problem. *Operations Research*, *28* (3-part-i), 628–632,

Ravi, R., & Salman, F.S. (1999). Approximation algorithms for the traveling purchaser problem and its variants in network design. *European symposium on algorithms* (pp. 29–40).

Real, L.B., Contreras, I., Cordeau, J.-F., de Camargo, R.S., de Miranda, G. (2021). Multimodal hub network design with flexible routes. *Transportation Research Part E: Logistics and Transportation Review*, *146*, 102188,

Reuters (2019). *BASF says it has prepared for any repeat of low Rhine water levels | Reuters.* Retrieved 2021-10-13, from https://www.reuters.com/article/us-basf-results-rhine/basf-says-it-has-prepared-for-any-repeat-of-low-rhine-water-levels-idUSKCN1S90LZ

Riera-Ledesma, J., & Salazar-González, J.J. (2005). The biobjective travelling purchaser problem. *European Journal of Operational Research*, *160* (3), 599–613,

Riessen, B.V., Negenborn, R.R., Dekker, R., Lodewijks, G. (2015). Service network design for an intermodal container network with flexible transit times and the possibility of using subcontracted transport. *International Journal of Shipping and Transport Logistics*, *7*(4), 457–478,

Roy, A., Maity, S., Moon, I. (2023). Multi-vehicle clustered traveling purchaser problem using a variable-length genetic algorithm. *Engineering Applications of Artificial Intelligence*, *123*, 106351,

Sabar, N.R., Goh, S.L., Turky, A., Kendall, G. (2021). Population-based iterated local search approach for dynamic vehicle routing problems. *IEEE Transactions on Automation Science and Engineering*, *19*(4), 2933–2943,

Sims, R., Schaeffer, R., Creutzig, F., Cruz-Núñez, X., D'Agosto, M., Dimitriu, D., ... Tiwai, G. (2014). *Transport. In: Climate Change 2014: Mitigation of Climate Change. Contribution of Working Group III to the Fifth Assessment Report of the Intergovern-mental Panel on Climate Change* (Tech. Rep.). United Kingdom and New York.

Singh, S.K., & Yadav, V. (2023). Modified goal programming approach for solving multi-objective environmental management problem. *Annals of Operations Research*, 1–17,

Smith, S.L., & Imeson, F. (2017). Glns: An effective large neighborhood search heuristic for the generalized traveling salesman problem. *Computers & Operations Research*, *87*, 1–19,

StatistischeBundesamt (2019). *Fachserie Binnenschifffahrt.* statistische Daten- bank, Fachserie Binnenschifffahrt (monatlich). Retrieved from gene- sis.destatis.de

SteadieSeifi, M., Dellaert, N.P., Nuijten, W., Van Woensel, T., Raoufi, R. (2014). Multimodal freight transportation planning: A literature review. *European journal of operational research*, *233*(1), 1–15,

Sun, Y., Hrušovskỳ, M., Zhang, C., Lang, M. (2018). A time-dependent fuzzy programming approach for the green multimodal routing problem with rail service capacity uncertainty and road traffic congestion. *Complexity*, *2018*, ,

Sundar, K., Venkatachalam, S., Rathinam, S. (2016). Formulations and algorithms for the multiple depot, fuel-constrained, multiple vehicle routing problem. *2016 american control conference (acc)* (pp. 6489–6494).

Tawfik, C., & Limbourg, S. (2019). A bilevel model for network design and pricing based on a level-of-service assessment. *Transportation Science*, *53*(6), 1609-1626,

ViaDonau (2012). *Handbuch der Donauschifffahrt.*

Vidal, T., Crainic, T.G., Gendreau, M., Lahrichi, N., Rei, W. (2012). A hybrid genetic algorithm for multidepot and periodic vehicle routing problems. *Operations Research*, *60*(3), 611–624,

Voß, S. (1996). Dynamic tabu search strategies for the traveling purchaser problem. *Annals of Operations Research*, *63*(2), 253–275,

Wang, C., Qin, F., Xiang, X., Jiang, H., Zhang, X. (2023). A dual-population based co-evolutionary algorithm for capacitated electric vehicle routing problems. *IEEE Transactions on Transportation Electrification*, 1-1, https://doi.org/10.1109/TTE.2023.3294588

Wang, Z., & Qi, M. (2019). Service network design considering multiple types of services. *Transportation Research Part E: Logistics and Transportation Review*, *126*, 1–14,

Wehrle, R., Wiens, M., Schultmann, F., Akkermann, J., Bödefeld, J. (2020). Ebenensystem zur resilienzbewertung kritischer verkehrsinfrastrukturen am beispiel der wasserstraßen. *Bautechnik*, ,

Wu, Y. (2021). A survey on population-based meta-heuristic algorithms for motion planning of aircraft. *Swarm and Evolutionary Computation*, *62*, 100844,

Xing, Z., & Tu, S. (2020). A graph neural network assisted monte carlo tree search approach to traveling salesman problem. *IEEE Access*, *8*, 108418–108428,

Xiong, G., & Wang, Y. (2014). Best routes selection in multimodal networks using multi-objective genetic algorithm. *Journal of Combinatorial Optimization*, *28*(3), 655–673,

Ye, J., Jiang, Y., Chen, J., Liu, Z., Guo, R. (2021). Joint optimisation of transfer location and capacity for a capacitated multimodal transport network with elastic

demand: a bi-level programming model and paradoxes. *Transportation Research Part E: Logistics and Transportation Review*, *156*, 102540,

Zameni, S., & Razmi, J. (2015). Multimodal transportation p-hub location routing problem with simultaneous pick-ups and deliveries. *Journal of Optimization in Industrial Engineering*, *8*(17), 11–20,

Zgonc, B., Tekavčič, M., Jakšič, M. (2019). The impact of distance on mode choice in freight transport. *European Transport Research Review*, *11*(1), 1–18,

Zhang, J., Ding, H.W., Wang, X.Q., Yin, W.J., Zhao, T.Z., Dong, J. (2011). Mode choice for the intermodal transportation considering carbon emissions. *Proceedings of 2011 ieee international conference on service operations, logistics and informatics* (p. 297-301).

Zhao, Y., Fan, Y., Zhou, J., Kuang, H. (2019). Bi-objective optimization of vessel speed and route for sustainable coastal shipping under the regulations of emission control areas. *Sustainability*, *11*(22), ,